LUMPED AND DISTRIBUTED MODELS OF THE ELLIDAÁR GEOTHERMAL FIELD, SW-ICELAND

Ivan Penev,
UNU Geothermal Training Programme,
Orkustofnun - National Energy Authority,
Grensasvegur 9,
108 Reykjavik,
ICELAND

Permanent address:
New Energy Sources,
Stud. grad, "V.Gentchev" 51,
Sofia,
BULGARIA

ABSTRACT

The drawdown, mass and heat transport in the Ellidaár geothermal reservoir are studied. A lumped model and a distributed model are discussed, describing the past and present state of the field, its behaviour, and predictions for future exploitation.

The lumped model is mainly based upon measured drawdown, flowrate, and mass and heat changes since the start of production in the field. A more complex and accurate distributed model gives a broader and more detailed picture of the reservoir. It also takes into account all physical properties of the fluid and porous media.

Although the models are very different in their complexity and approach to the problems discussed, both of them give results which match the measurements very well.

TABLE OF CONTENTS

1. INTRODUCTION

1.1 Purpose of the study

Having the honour to be granted a Fellowship by the UNU Geothermal Training Programme, the author of this study spent six months during the summer of 1990 in a special training course at the National Energy Authority in Reykjavik, Iceland. The course started with two months of lectures on various special subjects concerning all aspects of exploration, production and the use of geothermal energy around the world. It was followed by a ten day field trip to the main high and low temperature fields of Iceland. The special subsequent course in reservoir engineering consisted of:

- attending special lectures on modelling and reservoir engineering;
- a review and study of advanced papers and publications on modelling;
- taking part in field well tests;
- the collection and evaluation of the available data;
- practical work with different special programmes, created for a personal computer (PC);
- writing a general report on modelling the Ellidaár geothermal field.

The research study for making this report was carried out during the last two months of the special geothermal course. The author was carefully supervised by his advisers Dr. Snorri Pall Kjaran and Mr. Sigurdur Larus Holm throughout the specialized course period.

The main purpose of the course was to provide the author with the necessary knowledge and experience for later use in his home country.

1.2 Statement of the problem

The main objective of the present study can be stated as determining the drawdown, mass and heat responses of the Ellidaár geothermal reservoir to the exploitation of the last 22 years and constructing lumped and distributed models for describing its physical parameters and behaviour, as well as making some future predictions on the changes that may occur due to different production rates.

1.3 Outline of solution to the problem

In order to solve the problems concerning the modelling of the reservoir, all existing field data and measurement results were carefully studied. All available information on the geological, geophysical, hydrogeological and geochemical background of the area was also reviewed.

The main scope of the study is confined to calibrating the values of the reservoir parameters and getting the best fit with the measured field values of the drawdown, mass and heat transport. The obtained results were later used to create a model of the field that could be used for future predictions. Forecasts for the next ten years concerning the changes in water level, concentration of SiO_2 and temperature distribution in the field with different production conditions, are made. A great variety of problems were solved with the help of different PC programmes designed at Orkustofnun and by Vatnaskil Consulting Engineers. Simple programmes were also created during the special course. A Tulip personal computer was used for solving all the differential equations in the mathematical model, plotting the figures and writing the final report.

2. THE MAIN FEATURES IN THE ELLIDAÁR GEOTHERMAL FIELD

2.1 Locality

The Ellidaár low-temperature field (Figure 1) is located inside Reykjavik, in the southwestern part of Iceland. The area is situated close to the western part of the country's neo-volcanic zone, and especially close to the Krisuvik fissure swarm which extends out of it. The size of the real production area is very small - about 0.8 km².

2.2 Geology

The Ellidaár geothermal field lies mostly in Quaternary strata. Its main cover is of late Pleistocene olivine tholeite basalts. There is also an area covered by a postglacial lava flow from some 5,600 years ago. Faults and fractures are prominent features in the field (Tomasson, 1990).

The stratigraphical sequence can be divided into three main units (Tomasson et al., 1975). These are:

a) upper basalt unit, with thickness of not more than 400 m;
b) hyaloclastite unit, from 400 m down to 1000 m depth;
c) lower basalt unit, reaching from 1000 m down to 1800 m.

There is almost no alteration in the upper basalt unit, but in the deeper units, rocks are fairly altered (Smarason et al., 1989).
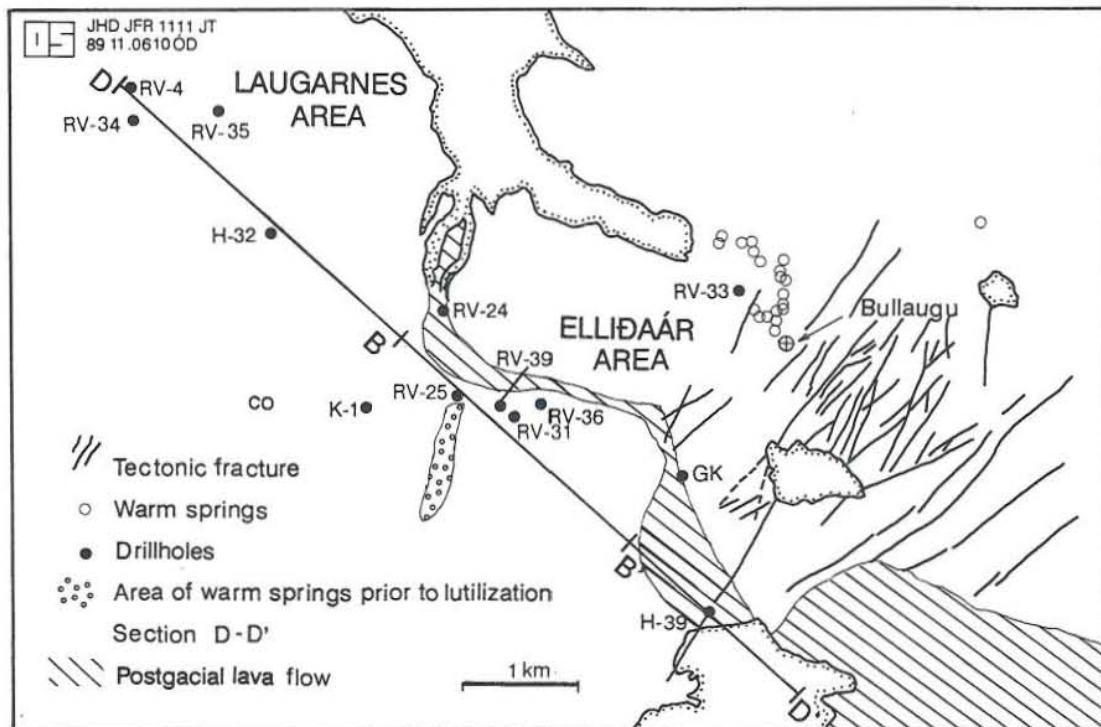
FIGURE 1: Low temperature geothermal areas in the Reykjavik region
showing main fissure direction (Tomasson, 1990)

2.3 Hydrogeology

There are two water systems in the area - a cold water system and a geothermal one. The main part of the cold water is located east of the geothermal area and reaches depths of about 800 - 1000 m. A smaller part of it is in the geothermal system itself, particularly in the uppermost and eastern parts of the area.

The geothermal aquifers are divided into three groups and follow the stratigraphical sequence. The uppermost aquifer is confined to the upper basalt unit and reaches down to 500 m depth with temperatures in the range of 40 to 90°C. Also in this unit is a cold water aquifer with a temperature of 20°C. The middle aquifer is confined to the hyaloclastite unit and its temperature reaches 100 - 110°C. The lowest aquifer is connected to the lower basalt unit and has a temperature range between 70 and 115°C. There are many faults and fissures crossing the whole geothermal system, thus creating an internal connection between the aquifers.

2.4 Geophysics

Through geophysical measurements and geological mapping, an anisotropy in a north to north-easterly direction is revealed, mainly in the central and northeastern part of the geothermal field (Figure 1). The resistivity measurements indicate a heavy infiltration of cold water at the outskirts of the volcanic zone to the south, and give evidence of a tighter formation to the north
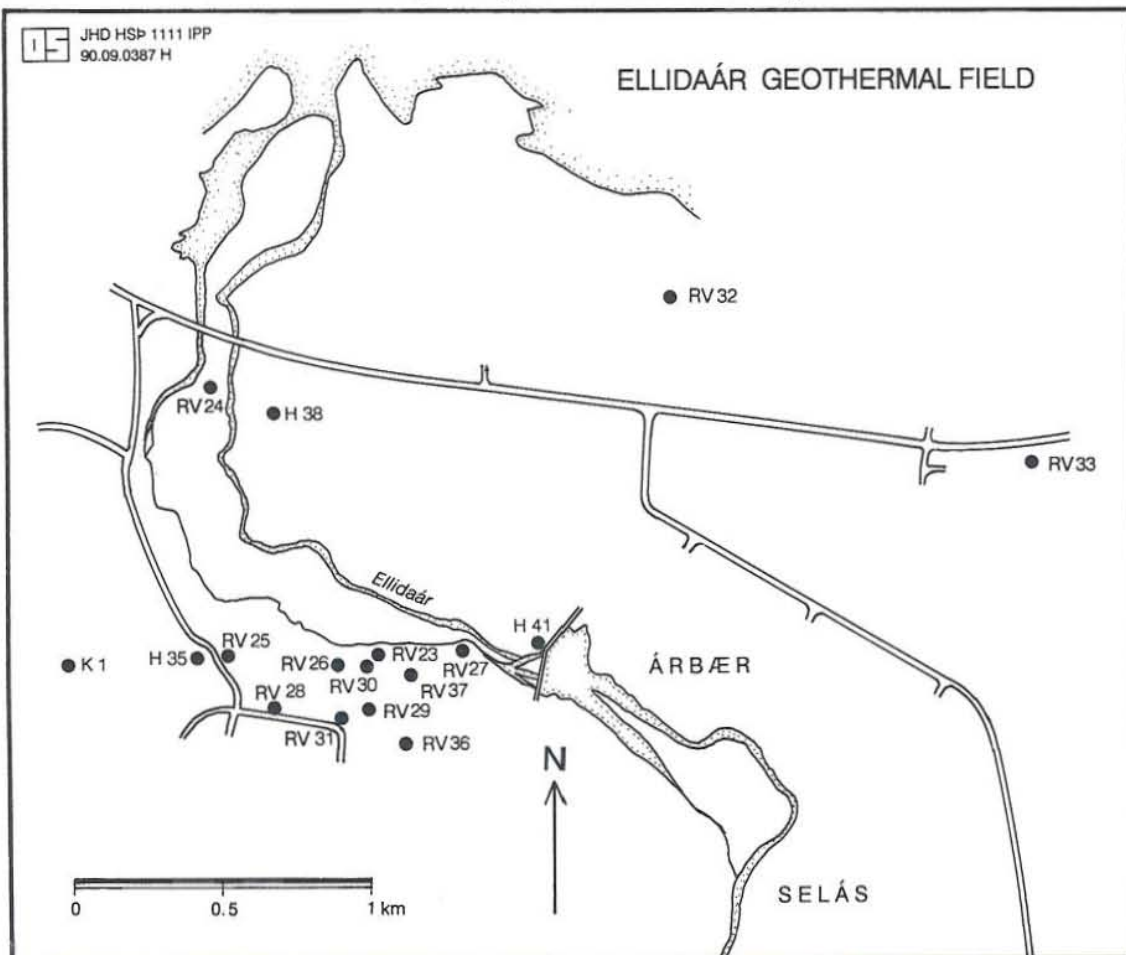
FIGURE 2: Location of wells
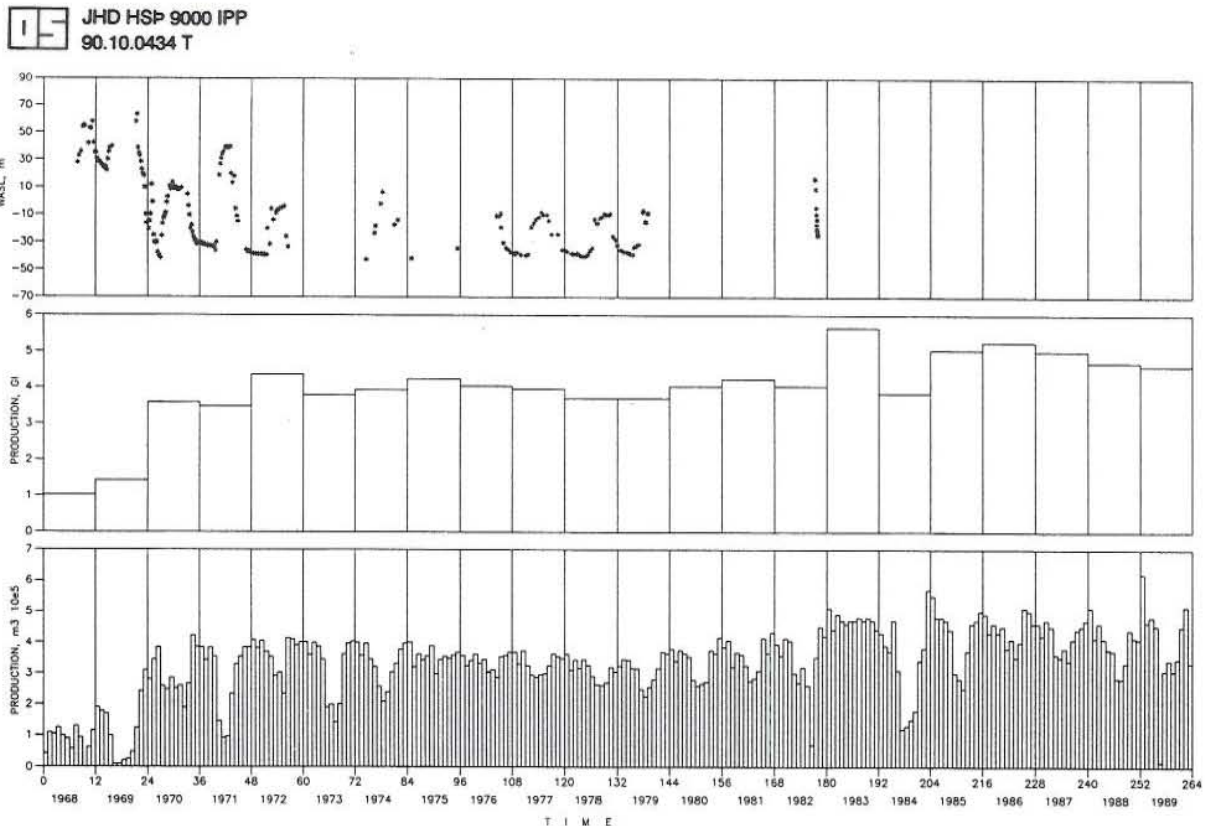
FIGURE 3: Production and drawdown history

(Tomasson et al., 1975; Georgsson, 1985). These measurements support the idea that the neo-volcanic zone could act as a constant head boundary condition for the Ellidaár geothermal field. On the other hand, no-flow boundary conditions are reached by approaching the impermeable, tighter formations in the western and northern part of the area (Kjaran, 1986).

2.5 Production history

The exploration of the Ellidaár geothermal reservoir began in 1967 with the drilling of the first wells in the area. Production from the field started the following year and since then, it has been one of the main sources of thermal water for the city of Reykjavik.

The production and drawdown history of the field can be seen in Figure 3. The average production for the period 1968-1989 is 126.3 l/s, and the total production from the area since the start of exploitation in 1968 is about 87 Gl. Production peak was reached in January 1989 (231.7 l/s), but the highest average yearly production (179.2 l/s) occurred in 1983 (Figure 4, Appendix: Table 1).

The initial water level in the reservoir dropped about 100 m almost immediately after commencing production. Since then it shows the same seasonal variations as the municipal demand for hot water. The biggest drawdown (190 m) measured in observation well RV-27 was observed in January 1989, but it exceeded 200 m in the centre of the production area. Thus, the specific yield is about 1.25 l/s/m.

Several tables including information about the production and results of calculations are in an Appendix which is published separately (see Penev, 1990).
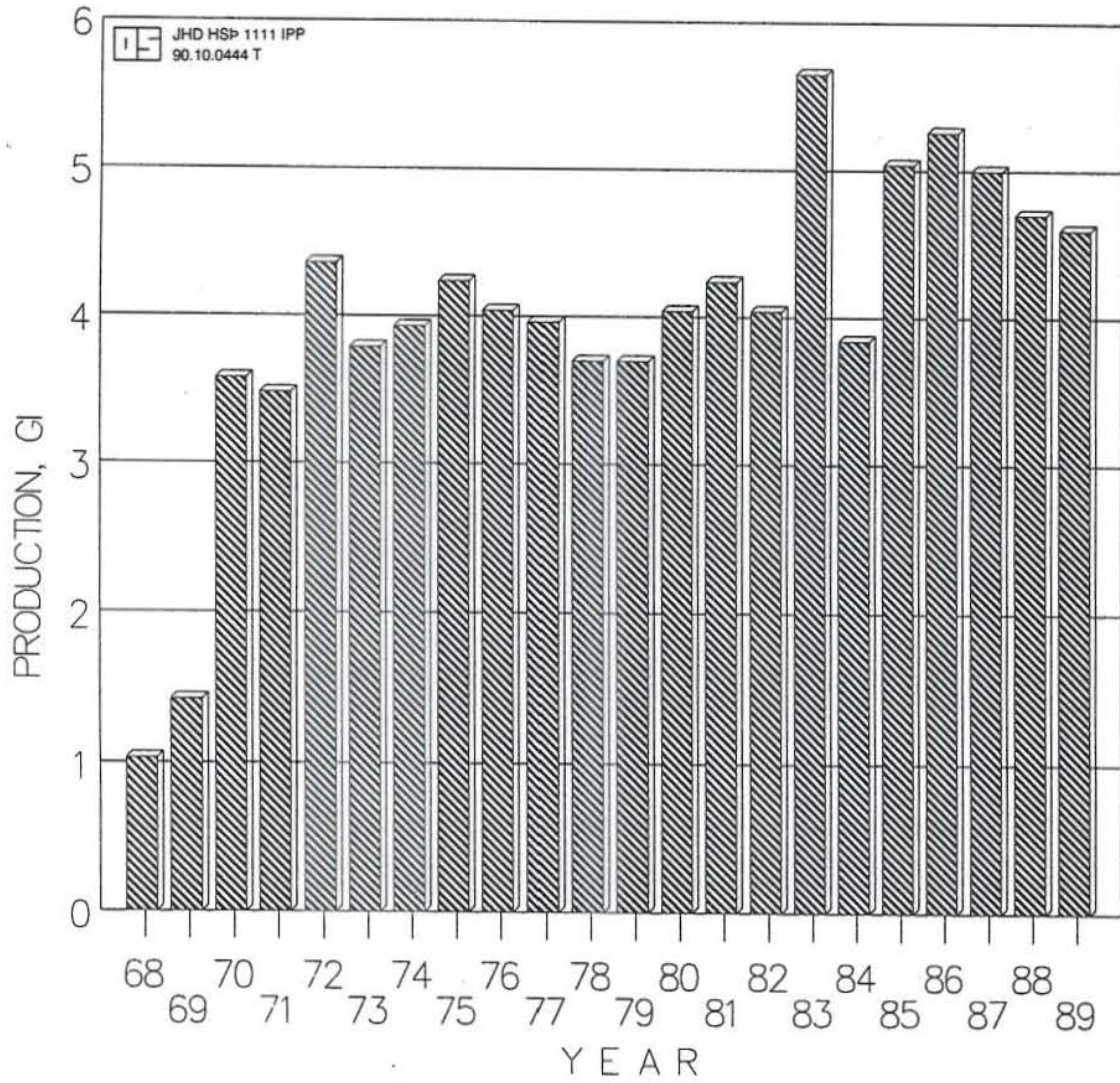
FIGURE 4: Annual production from the field

3. MODELLING OF THE ELLIDAÁR GEOTHERMAL FIELD

3.1 Need of a model

The optimal production strategy of a geothermal field cannot be obtained without using a good performing reservoir model. It should give a clear picture about all physical, chemical and reservoir parameters, and the obtained results should be comparable to those of field measurements. The past, present and future exploitation of the geothermal field must be in compliance with the created model. All plans for changing the production rate from the reservoir should be carefully checked with it. The drilling of new boreholes, their situation and casing design, possible reinjection options for recovering the water level, changes of the chemical concentration and heat losses due to interaction with another aquifer should be taken into consideration, only after addressing the reservoir model. As a final result, it should reward its users with the best economical solution for their needs.

3.2 The lumped model

3.2.1 General description of the model

This is the simplest model used for simulation of pressure response data. Usually it describes the response and behaviour of the geothermal reservoir in terms of only a few parameters. It does not take into account the internal distribution of mass and energy; attention is restricted entirely to the system itself and to what crosses the boundaries. Figuratively speaking, a lumped model uses 2 (or 3) blocks to represent the entire system (Figure 5). One of the blocks is the main production reservoir and the other acts as a recharge one. As time is the only independent variable, the model is usually solved by ordinary differential equations representing mass and energy conservation (Kjaran and Eliasson, 1983).
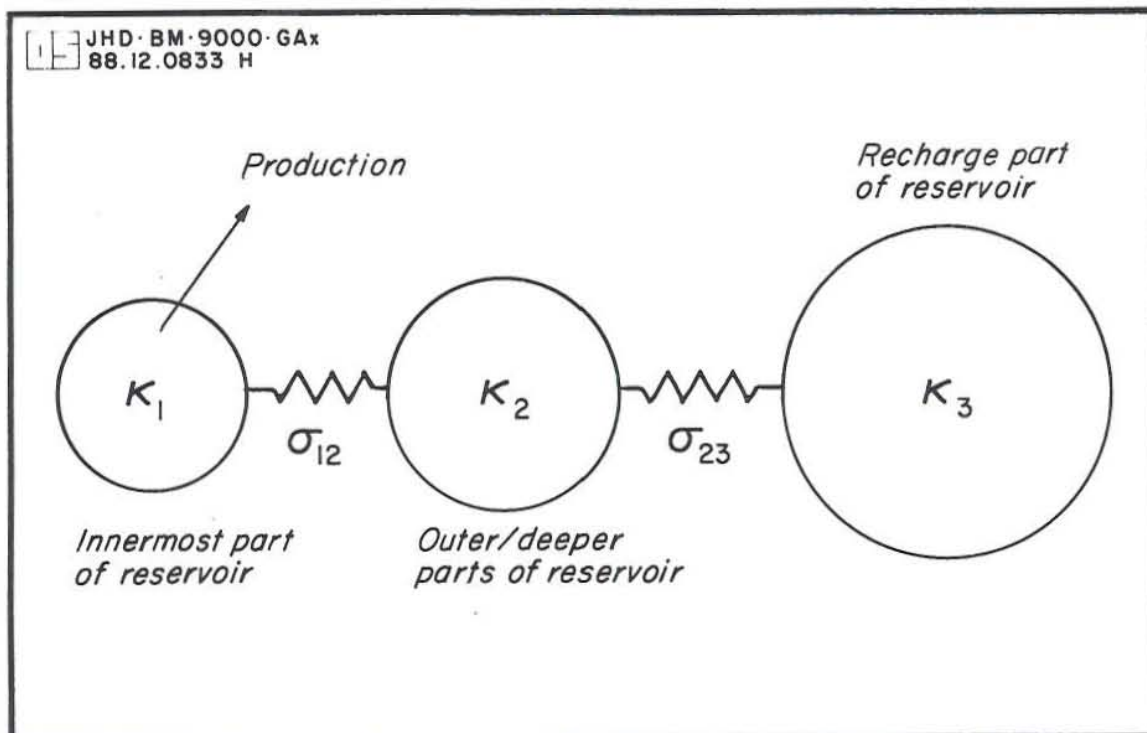
FIGURE 5: General idea of the lumped model (Axelsson, 1989)
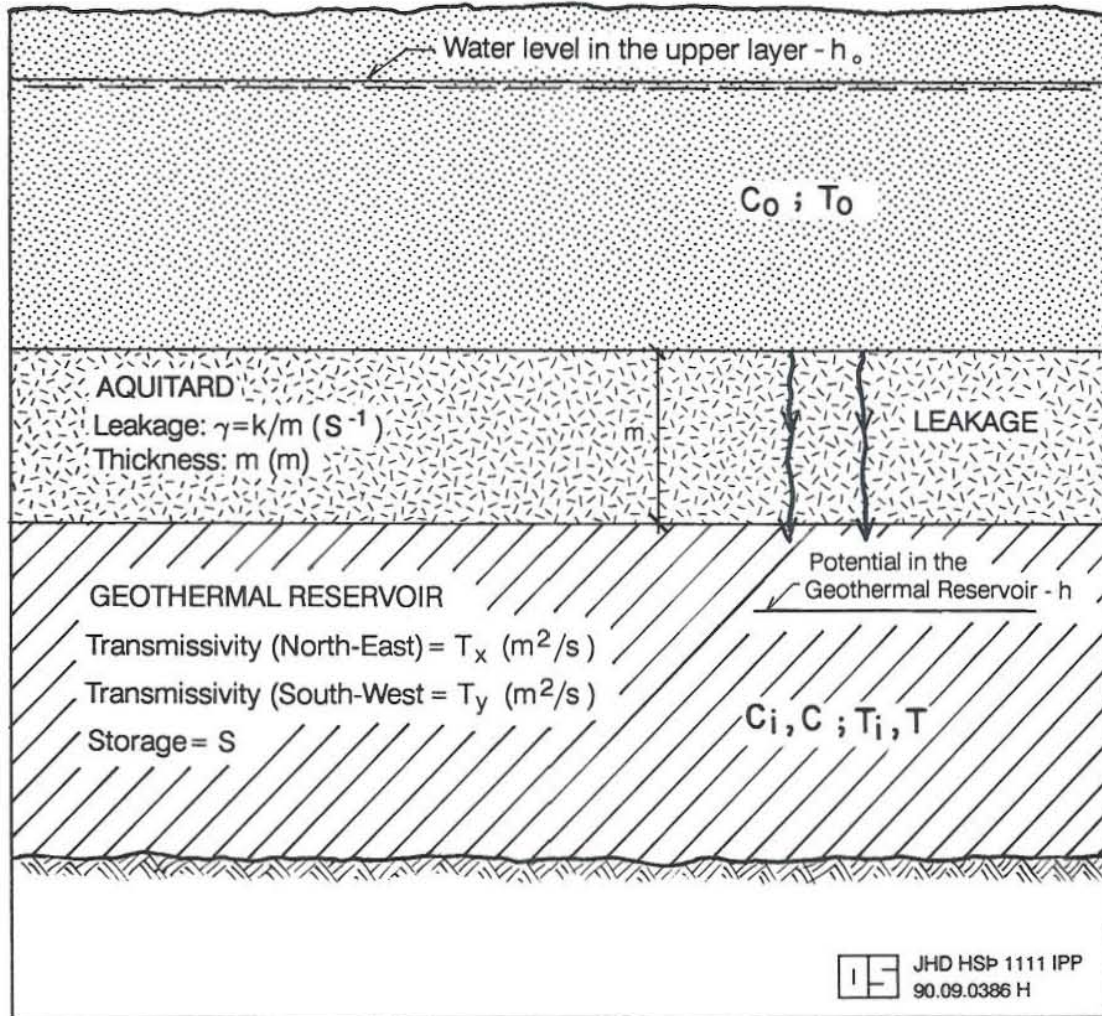
FIGURE 6: A simple geological cross-section of the Ellidaár field

The advantage of these models is their relative simplicity and easy operation. The methods tackle simulation as an inverse problem, do not need very complicated programming and could be solved in a short period of time. Usually, they are used as a first stage in a modelling process and for checking the results of more complex modelling.

The main disadvantage of the lumped models is that they do not consider fluid flow within the reservoir, and do not take into account the spatial variations in reservoir properties and conditions.

3.2.2 Theory and mathematical background

For this method of data simulation, some measurement field data is usually required: reservoir pressure response $p(t)$ and rate of production $q(t)$. After choosing an appropriate lumped model, an initial guess for the model parameters is made. To fit its theoretical response to the field data,

an automatic, iterative non-linear least square technique is then used. It requires less time than for more complex numerical modelling (Axelsson, 1989). In the next chapters the mathematical approach for flow, mass and heat transport is presented.

3.2.2.1 Flow equation

As stated previously, the Ellidaár geothermal reservoir underlies a cold aquifer containing fresh water. Between them, there is a semi-permeable aquitard which confines the thermal water as can be seen in Figure 6. These three layers have different hydraulic, chemical and temperature properties, which are taken into account in the lumped model.

The continuity of the mass can be written as:

$$Q = \frac{Ak}{m}(h_o - h) - AS\frac{dh}{dt} \quad , \tag{1}$$

$$s = h_o - h \quad , \tag{2}$$

$$\frac{ds}{dt} + \frac{k}{Sm}s = \frac{Q}{AS} \quad , \tag{3}$$

where
Q : average production, m^3 /s;
A : area, m^2 ;
S : storage coefficient;
m : thickness of the aquitard, m;
k : permeability of the aquitard, m/s;
s : drawdown, m;
h_o : potential in the upper layer, m;
h : potential in the geothermal reservoir, m.

The timeconstant is defined by:

$$K = \frac{mS}{k} \quad , \tag{4}$$

$$\frac{ds}{dt} + \frac{1}{K}s = \frac{Q}{AS} \quad . \tag{5}$$

The convolution approach with the superposition principle is used to solve the equation:

$$s(t_i) = \sum_{i=1}^{k}(Q_i - Q_{i-1})F(t_k - t_{i-1}) \quad . \tag{6}$$

With a constant pumping rate (Q = const.) and $t \rightarrow \infty$, the stationary water level is given by:

$$s_{st} = \frac{KQ}{AS} \ . \tag{7}$$

The unit response function F(t) is given by:

$$F(t) = C_f(1 - e^{-t/K}) \ . \tag{8}$$

3.2.2.2 Mass transport

The continuity of concentration is given by:

$$QC = qC_o - Ab\phi \frac{dC}{dt} + q_oC_i \ , \tag{9}$$

with

$$q = \frac{Ak}{m} s = Q(1 - e^{-t/K}) \ , \tag{10}$$

where
C	:	concentration in the geothermal reservoir, mg/l;
C_o	:	concentration in the upper layer, mg/l;
C_i	:	initial concentration in the geothermal reservoir, mg/l;
b	:	thickness of the geothermal aquifer, m;
ϕ	:	porosity of the geothermal aquifer;
q_o	:	natural flow into the geothermal aquifer, m³ /s.

Equation 9 can now be transformed to:

$$\frac{dC}{dt} + \frac{CQ}{Ab\phi} = \frac{C_oQ}{Ab\phi} (1 - e^{-t/K}) + \frac{q_o}{Ab\phi} C_i \ . \tag{11}$$

With Q = constant, for the concentration's timeconstant we get:

$$K_c = \frac{Ab\phi}{Q} \ . \tag{12}$$

For the current concentration in the geothermal aquifer we get:

$$C = C_i e^{-t/K} + (C_o + \frac{q_o}{Q} C_i)(1 - e^{-t/K}) \tag{13}$$

Solving Equation 9, assuming t → ∞, and taking the initial values for C_o and C_i and the average production rate, we can calculate the recharge (q_o) into the system:

$$q_o = \frac{(C - C_o)Q}{C_i} \ . \tag{14}$$

3.2.2.3 Heat transport

For continuity of heat, the following differential equations are used:

$$\rho_w c_w T_o q - ((1 - \phi)\rho_s c_s + \phi\rho_w c_w)Ab \frac{dT}{dt} + q_o T_i = \rho_w c_w TQ \ , \tag{15}$$

where

$$q = \frac{Ak}{m} s = Q(1 - e^{-t/K}) \ , \tag{16}$$

and

T   : temperature in the geothermal aquifer, °C;
T_i : initial temperature in the geothermal aquifer, °C;
T_o : temperature in the upper aquifer, °C;
$c_s \& c_w$: heat capacity of the solid matrix and water, kg/m³ ;
$\gamma_s \& \gamma_w$: density of the solid matrix and water, kg/m³ ;

and the retardation coefficient (R_h):

$$R_h = (1 + \frac{(1 - \phi)\rho_s c_s}{\phi\rho_w c_w}) \ . \tag{17}$$

Equation 15 is transformed to:

$$\frac{dT}{dt} + \frac{TQ}{Ab\phi R_h} = \frac{T_o Q}{Ab\phi R_h} (1 - e^{-t/K}) + \frac{q_o}{Ab\phi R_h} T_i \ . \tag{18}$$

For the temperature timeconstant we get:

$$K_T = \frac{Ab\phi R_h}{Q} \ . \tag{19}$$

The temperature in the geothermal reservoir can be calculated by:

$$T = T_i e^{-t/K} + (T_o + \frac{q_o}{Q} T_i)(1 - e^{-t/K}) \ . \tag{20}$$

For calculating the final results and determining the field parameters, simple programmes for a PC were made and used.

3.2.3 Model test and results

To evaluate the merits and reliability of the proposed lumped model, the above stated equations were used for calculating: a) drawdown; b) mass transport; c) heat transport. As input data, the production flowrate and water level field measurements from observation well RV-27 were used. That data was provided by the Reykjavik District Heating Service and the Vatnaskil Consulting

Engineers (1982a; 1982b). The obtained results are stated below.

3.2.3.1 Drawdown performance

As can be seen in Figure 7, the unit response function (URF) shows that steady-state conditions had been reached 12 days after the start of production. The value of URF is 0.833 m/(l/s) which gives a specific yield of 1.2 l/s/m. This indicates a recharge either from hot water with lateral flow, or cold vertical recharge from the above lying aquifer. In fact both effects are taking place, but as the chemical and temperature measurements show, the second is more strongly represented. This is, in fact, leakage through the semi-permeable layer due to the lowering of the water level of the geothermal reservoir.

The calculated water level fits very well with the measured one, in terms of seasonal variations. A minor difference is observed in the amplitude: the oscillations produced from the lumped model have bigger peaks and bottoms than the measured oscillations (Figure 8).

The forecast for the next ten years (till year 2000) is then made, showing the eventual change of the water level with a change in production rate. The present water level of about 35 m below sea level (corresponding to a drawdown of 110 m) will be kept, if production does not exceed an average of 147 l/s per year (Figure 8). Other predicted flow rates will either decrease or increase the water level (Appendix: Table 2).
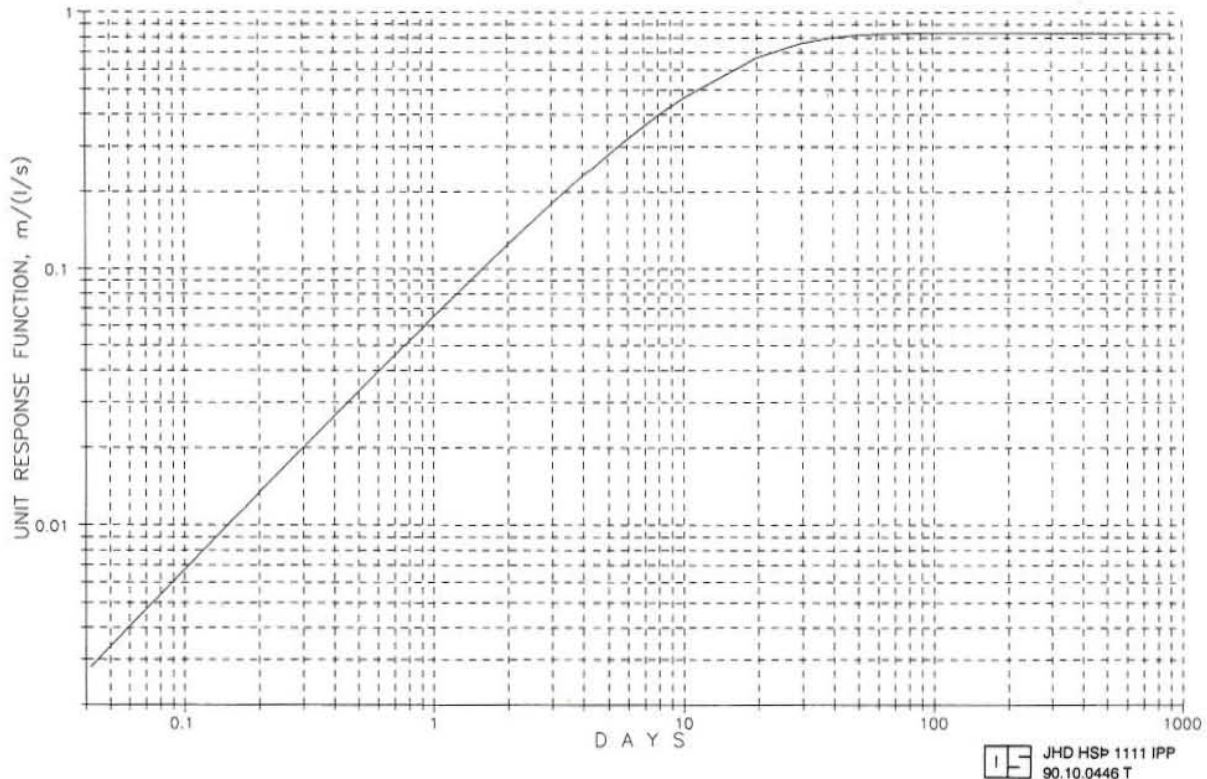
FIGURE 7: Unit response function
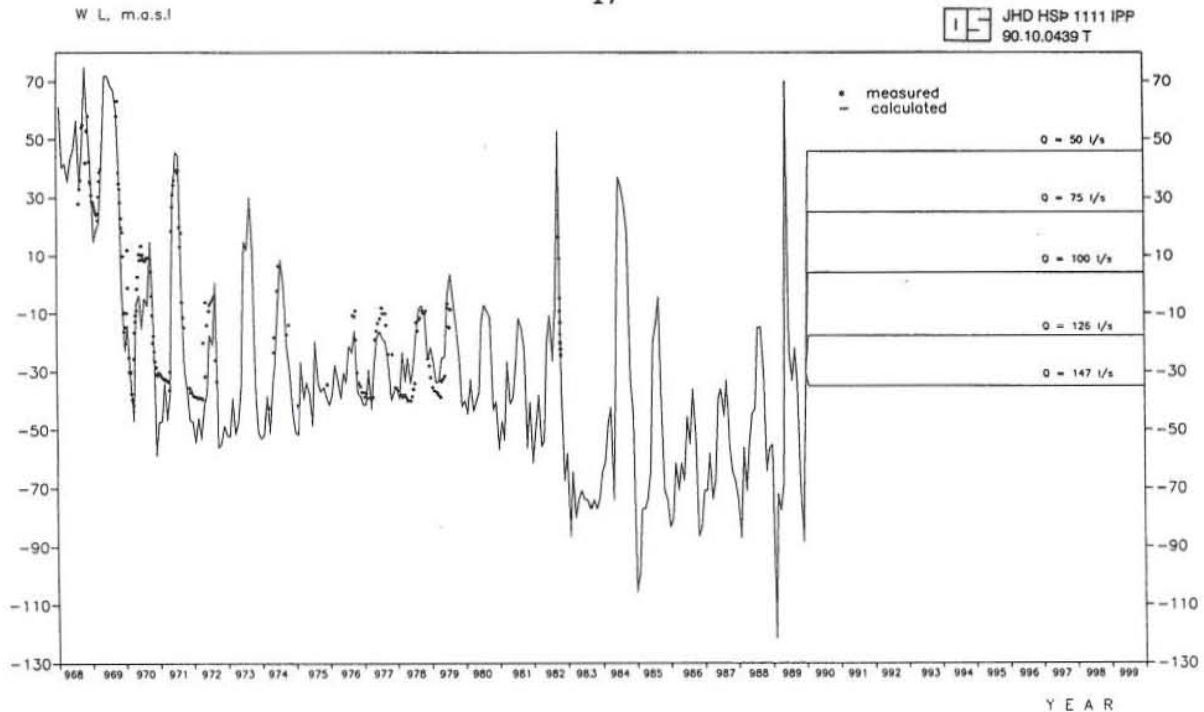
FIGURE 8: Prediction of the water level with different production for the next 10 years

The calibration parameters k, m and A can be calculated, assuming that the storage coefficient in the production area is given as $S = 1.6 \times 10^{-3}$:

$$k = 1.5 \times 10^{-7} \text{ m/s}, \quad m = 100 \text{ m}, \quad A = 0.8 \text{ km}^2$$

3.2.3.2 Mass transport

The measurements made in the observation well RV-27 speak for a change of the SiO_2 content in the thermal water. Again, the reason is the lowering of the water level in the main geothermal reservoir. Because of the greater value of the timeconstant for mass transport, smaller changes in the calculated values are observed compared to the drawdown (Figure 9). But the decline of the silica concentration is obvious: it goes from 140 mg/l - to 71 mg/l (Appendix: Table 3). The calculated values are close to those measured.

Using Equation 12 with average constant production through the whole calibration period (Q = 126 l/s), the calibrating parameters b and ϕ can be calculated, assuming that the area (A) is already known:

$$b = 1000 \text{ m}; \quad \phi = 0.1$$

Similar predictions as for the drawdown, can also be made for the mass transport. From Table 4 in the Appendix, it can be seen how the consequent future change of production could affect the SiO_2 change content. These results are summarized in Table 1.

It is obvious that the decline will continue if production is kept to the current level. From Equation 13 we can calculate at what production rate (Q) the concentration of SiO_2 will remain at its present value - 71.17 mg/l. We can also determine the time (t) for reaching the initial reservoir concentration of 140 mg/l (Figure 11) if production from the field stops, and natural recharge into it remains
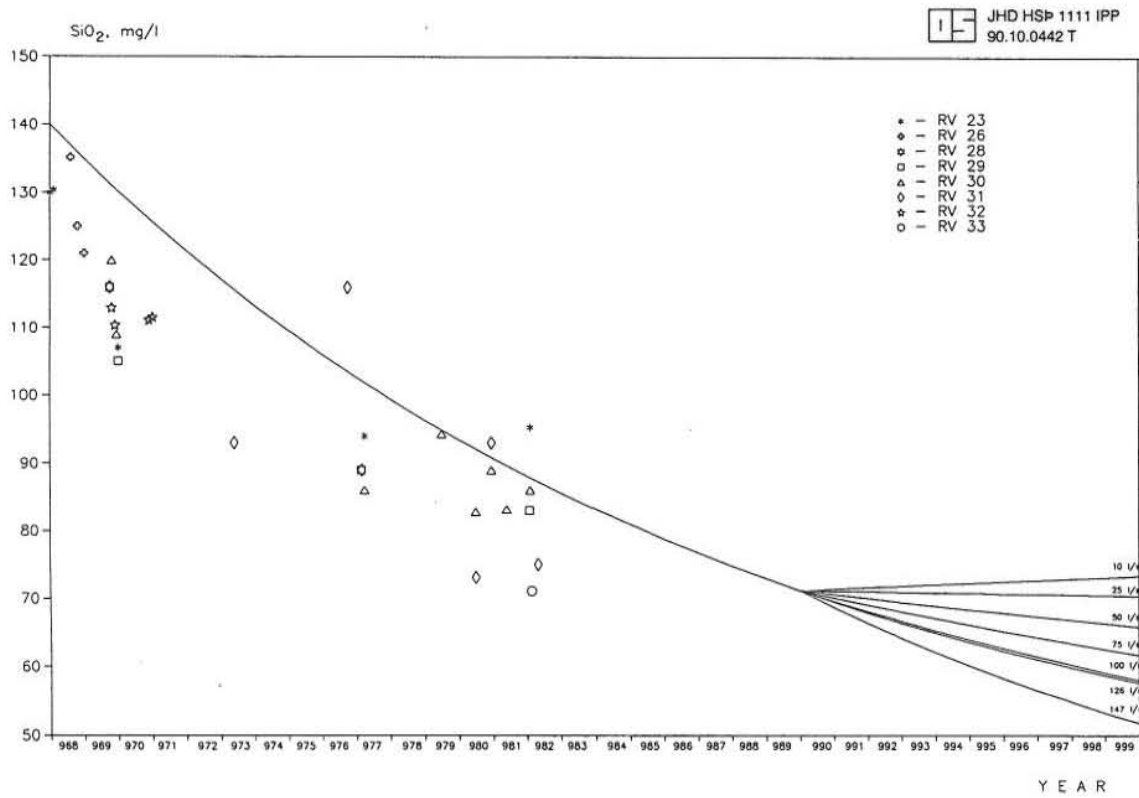
FIGURE 9: Mass transport, with prediction till the year 2000

TABLE 1: Predicted SiO_2 content for the year 2000 for different annual production values

Av. annual prod. (l/s)	SiO_2 in year 2000 (mg/l)
147	51.81
126	57.61
100	57.99
75	61.71
50	65.83
25	70.37
10	73.32

unchanged - q_o = 15 l/s. The last value we get from Equation 14, assuming that with time $t \to \infty$, the reservoir concentration of SiO_2 will reach 30 - 40 mg/l.

$$Q = 21 \text{ l/s}, \quad t = 162 \text{ years}$$
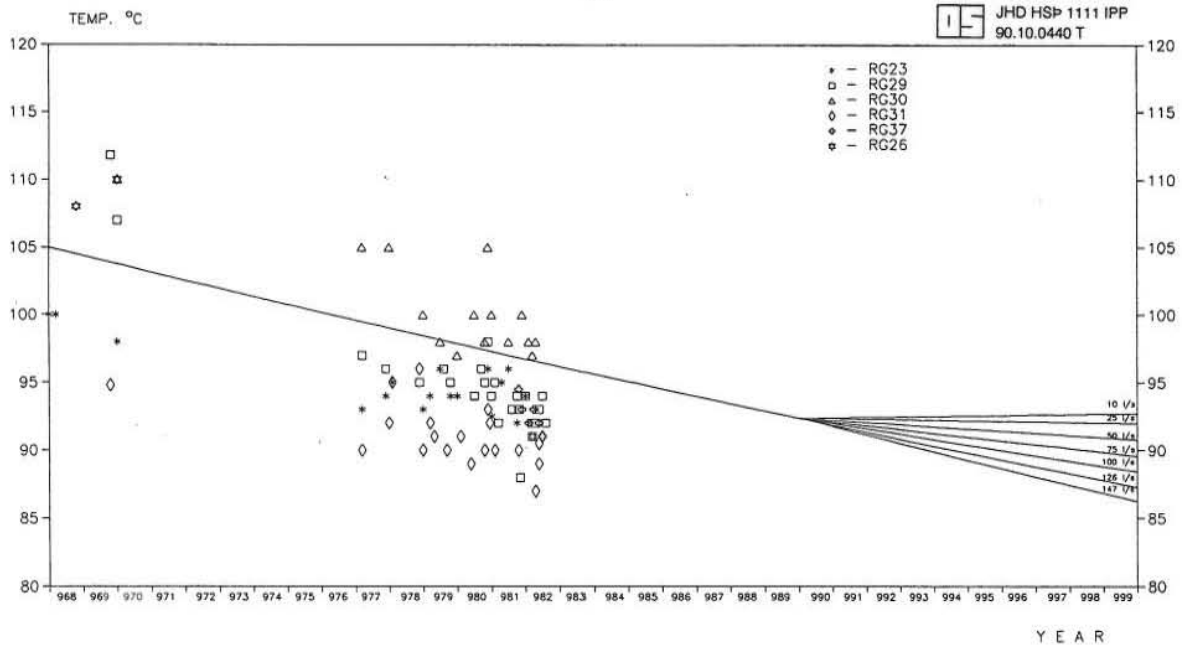
FIGURE 10: Heat transport, with prediction till year 2000

3.2.3.3 Heat transport

Due to exploitation of the geothermal field and the resulted lowering of the water level, a temperature decline is also observed: the initial temperature has dropped from 105°C to 92°C. This fits quite well with the observations made in all the wells in the field. As the timeconstant for temperature is bigger because the retardation coefficient (R_h = 6.6) is added, this decline is not so great as in the mass transport. Figure 10 and Table 3 in the Appendix show that the reduction of the initial temperature is in the range of 12-13°C.

The heat change for the next 10 years can be seen in Table 5 in the Appendix. It gives the temperature change during the prediction period with different production rates. The results for the year 2000 are summarized in Table 2.

TABLE 2: Predicted temperature in the year 2000 for different annual production values

Av annual prod. (l/s)	Temp. in year 2000 (°C)
147	86.26
126	87.29
100	88.42
75	89.57
50	90.76
25	91.97
10	92.70

With Equation 20 we can calculate at what production rate (Q) the current reservoir temperature of 92.37°C will remain unchanged, and when the initial temperature value (t) of 105°C will be reached,
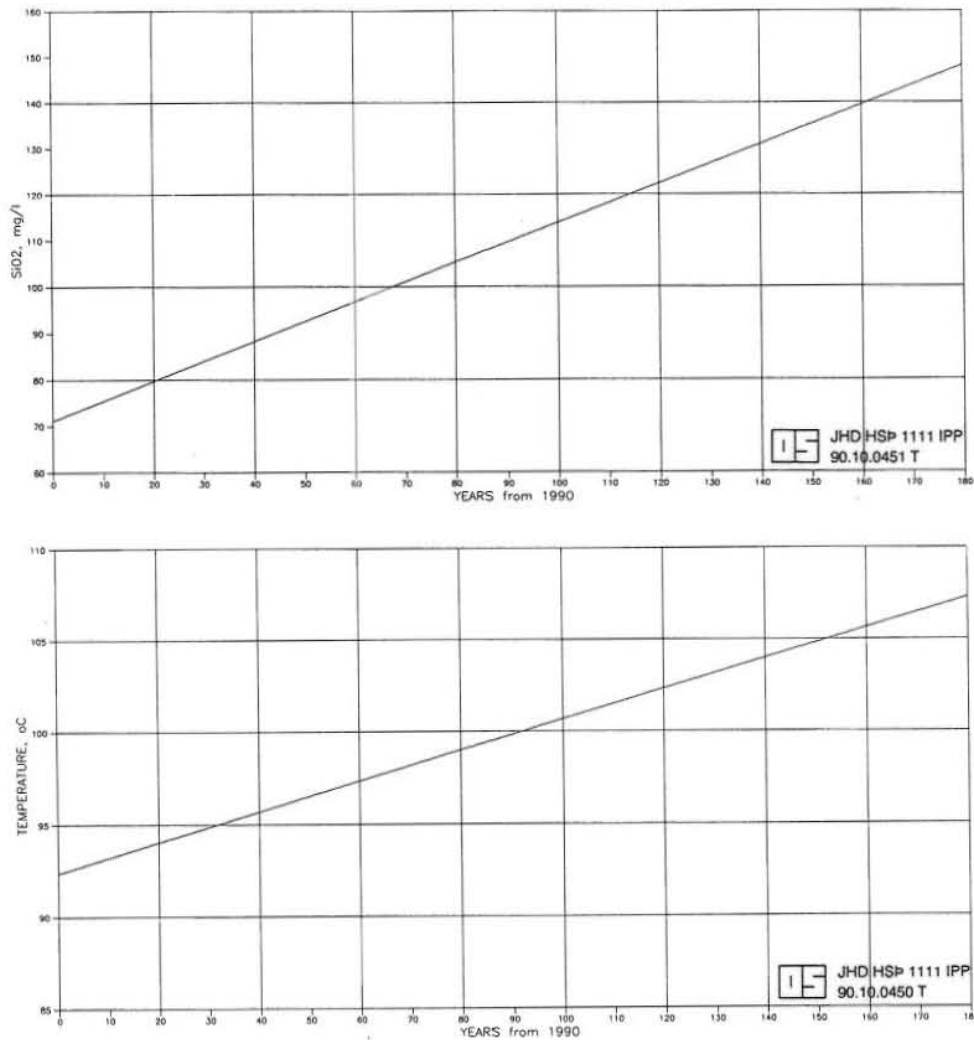
FIGURE 11:   Mass and heat recovery with no production from the field

assuming that production stops and the recharge into the reservoir remains constant -q_o = 15 l/s (Figure 11):

$$Q = 17 \text{ l/s}, \quad t = 153 \text{ years}$$

3.3   Distributed model

3.3.1   General description of the model

Distributed parameter models can be used for the simulation of geothermal reservoirs with many gridblocks. Their main advantage over the lumped models is that they take into account all spatial variations and changes in the thermodynamic conditions and reservoir parameters. As it is possible to create a finer mesh, those models could simulate not only flow, phase and thermal fronts, but the entire geothermal system including the reservoir's geometry, caprock, bedrock, cold aquifers, recharge zones, etc. The main disadvantage of the distributed models is that for this kind of simulation, there is always a need for big and complicated computer programmes and an experienced modeller (Bodvarsson and Witherspoon, 1989).

3.3.2 Theory and mathematical background of AQUA

The distributed model for the Ellidaár geothermal reservoir is made with the help of the AQUA programme designed by the Vatnaskil Consulting Engineers in Reykjavik (1989) and used specifically for flow and transport modelling. It is based on equations using the Galerkin finite element method.

The differential equation that forms the basis for the mathematical model subsequently solved by AQUA, can be written as:

$$a \frac{du}{dt} + b_i \frac{d}{dx_i} + \frac{d}{dx_j}\left(e_{ij}\frac{du}{dx_j}\right) + fu + g = 0 \tag{21}$$

3.3.2.1 Flow model

The transient flow problems are solved by AQUA as Equation 21 is reduced to:

$$a \frac{du}{dt} + \frac{d}{dx_i}\left(e_{ij}\frac{du}{dx_j}\right) + fu + g = 0 \tag{22}$$

Two boundary conditions are used:

a)   Dirichlet boundary condition. It prescribes the groundwater level, the piezometric head or the potential function at the boundary;

b)   Von Neuman boundary condition. It gives the flow at the boundary, which can be modelled by putting pumping sources at the no-flow boundary nodes.

In the case of the Ellidaár reservoir model, the following conditions were met:

- flow boundary from south and southeast;
- no-flow boundary elsewhere;
- anisotropy angles: a) 60° - in the southern and southeastern parts; b) 90° - in the northern and northeastern parts; c) 120° - in northwestern part of the field;
- anisotropy of the whole area - sqrt(T_{yy}/T_{xx}) = 0.3;
- initial values for transmissivity, storage and leakage coefficients are taken from field experience in the Ellidaár and neighbouring geothermal fields.

3.3.2.2 Mass transport model

Using main Equation 21 and choosing the proper parameters, AQUA is also designed to solve the mass transport problem. When the transient mass transport is handled, the main variables are defined as follows:

$$u = C$$

$$a = \phi b R_h$$

$$b_i = V_i b$$

$$e_{ij} = -\phi b D_{ij}$$

$$f = \phi b R_h \lambda + \gamma + Q$$

$$g = -\gamma C_o - Q C_w$$

(23)

where the dispersion coefficients D_{xx} and D_{yy} are defined as:

$$\phi D_{xx} = a_L V^n + D_m \phi$$

$$\phi D_{yy} = a_T V^n + D_m \phi$$

(24)

The retardation coefficient R_h is given by:

$$R_h = 1 + \beta(1 - \phi)\rho_s/(\phi\rho_w)$$

(25)

$$\beta = k_d \rho_w$$

(26)

The parameter γ is defined in the following way:

$$\gamma = (k/m)(h_o - h)$$

(27)

3.3.2.3 Heat transport model

In a similar way, AQUA is able to solve single phase heat transport problems by proper selection of the parameters for Equation 21. They must be defined as follows:

$$u = T$$

$$a = \phi b R_h$$

$$b_i = V_i b$$

$$e_{ij} = -b K_{ij}$$

$$f = \gamma + Q$$

$$g = -\gamma T_o - Q T_w$$

(28)

The heat dispersion coefficients are given by:

$$K_{xx} = a_L V^n + D_m \phi$$

$$K_{yy} = a_T V^n + D_m \phi$$

(29)

The heat retardation coefficient R_h is given by:

$$R_h = 1 + \beta(1 - \phi)\rho_s/(\phi\rho_w)$$

(30)

$$\beta = \frac{c_s}{c_w} \tag{31}$$

3.3.3 Results from the distributed model

3.3.3.1 Flow problem

The modelling starts by assuming values for the main reservoir parameters such as transmissivity, storage coefficient, leakage coefficient, anisotropy, etc., which are close to values from neighbouring geothermal fields and Ellidaár itself. The modelled area is somewhat greater than the actual production zone, but the aim is to observe whether bigger production values from the modelled geothermal reservoir could eventually affect the adjacent fields (Figure 12).
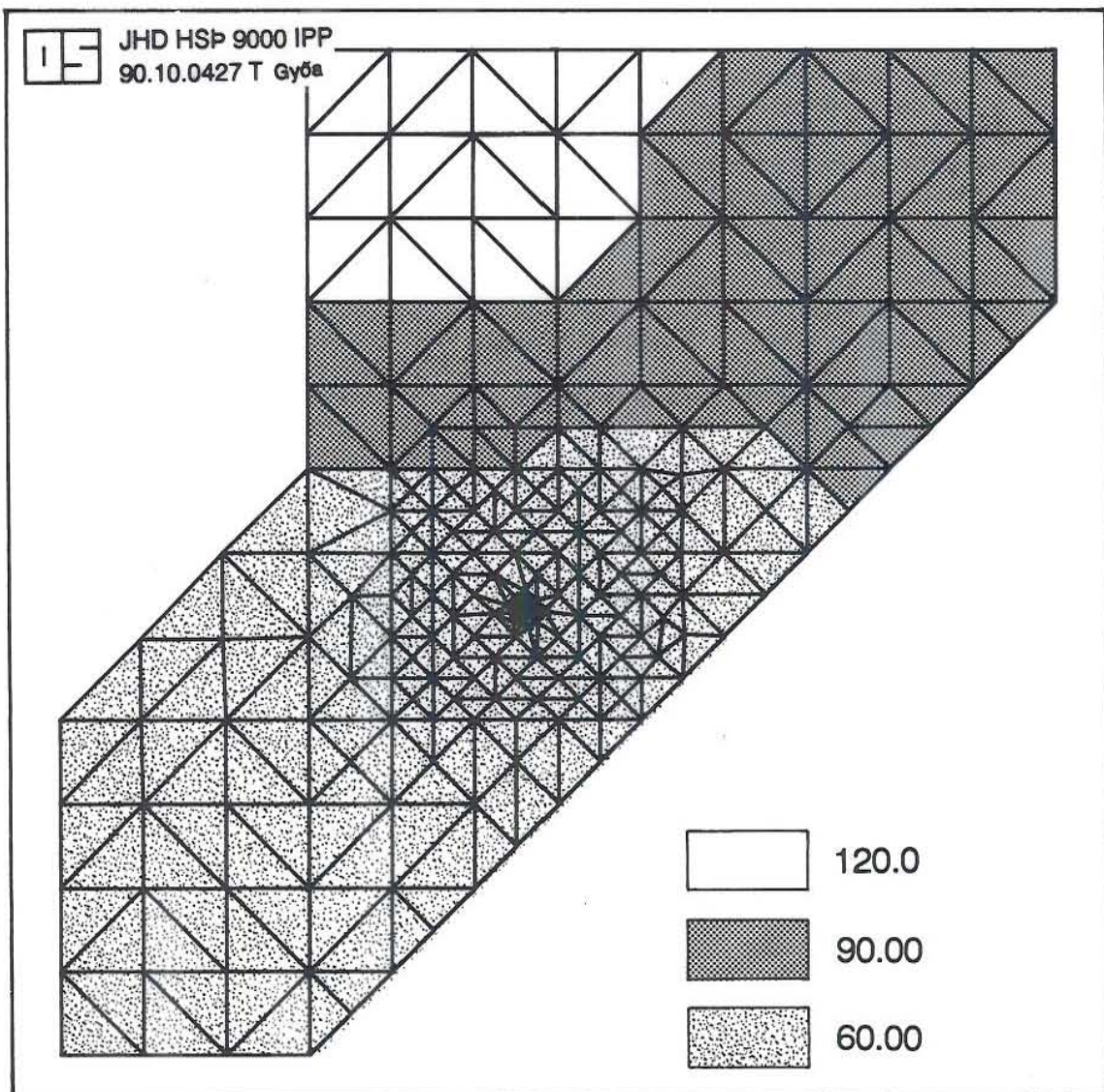
FIGURE 12: Boundaries and anisotropy direction
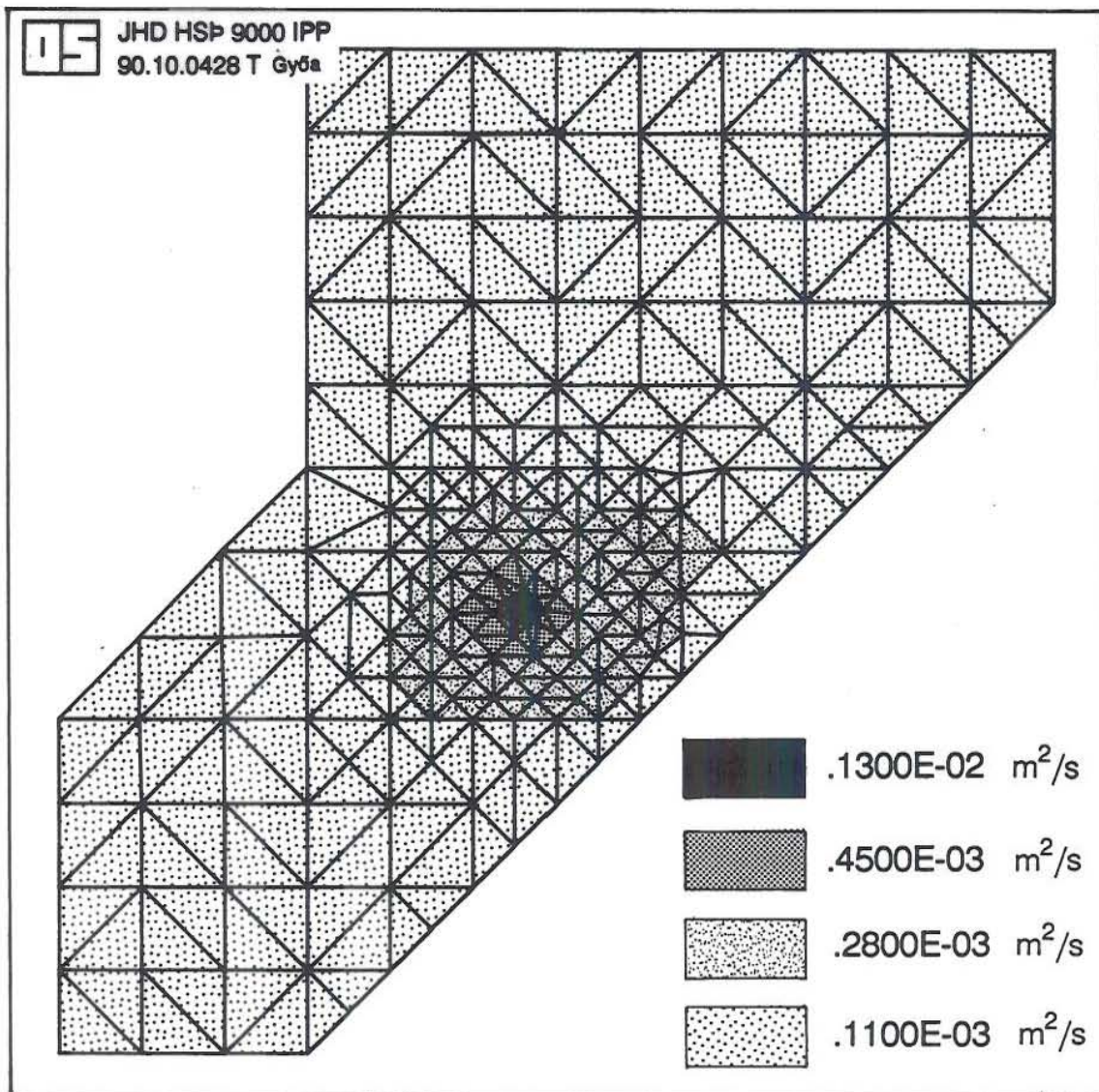
FIGURE 13: Map for transmissivity

The values of the main parameters are shown in Figures 13, 14 and 15. In the vicinity of the production zone they are as follows:

Transmissivity T_{xx} = 1.3×10^{-3} m² /s

Transmissivity T_{yy} = 1.3×10^{-4} m² /s

Storage coefficient S = 1.4×10^{-4}

Leakage coefficient k/m = 1.7×10^{-9} s^{-1}

Anisotropy $\sqrt{(T_{xx}/T_{yy})}$ = 0.3
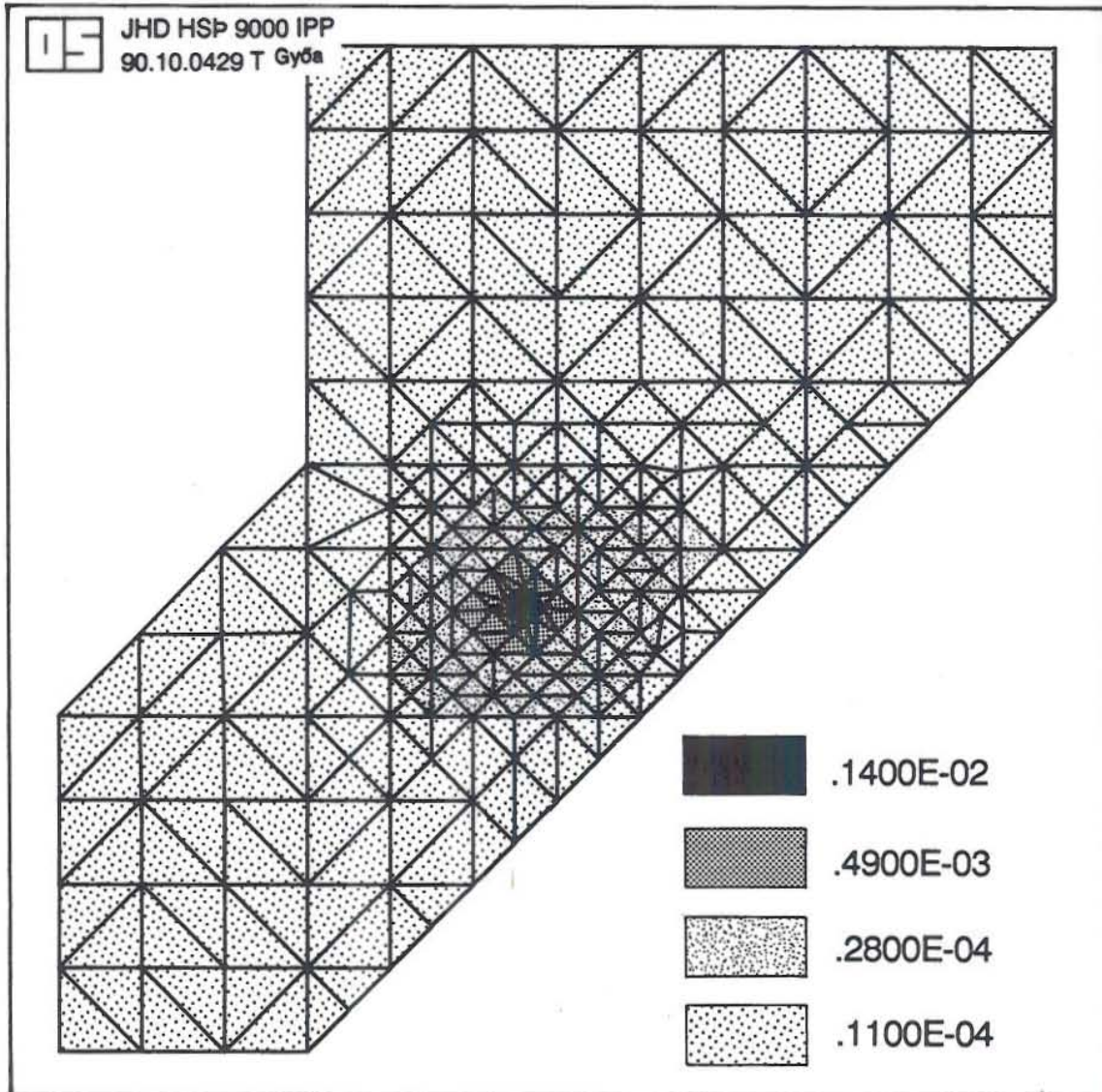
FIGURE 14: Map for storage coefficient

The model corresponds very well with the field measurements and the calculations done by the lumped model. The only slight difference is in the amplitude of the curves, especially during periods of high and low production values (Figure 16).

Calculations made by the AQUA programme show that the amount of thermal water flowing through the boundary around the production zone (0.2 km^2) is $q_l = 111$ l/s and the amount due to leakage is about 15 l/s. Only 0.1 l/s flows through the outer boundaries (Appendix: Table 6).

The aerial distribution of the drawdown (Figure 17), and the cross-section across the whole field in a southwest - northeast direction (Figure 18) show that the extraction of the thermal water affects only a small area around the production wells.
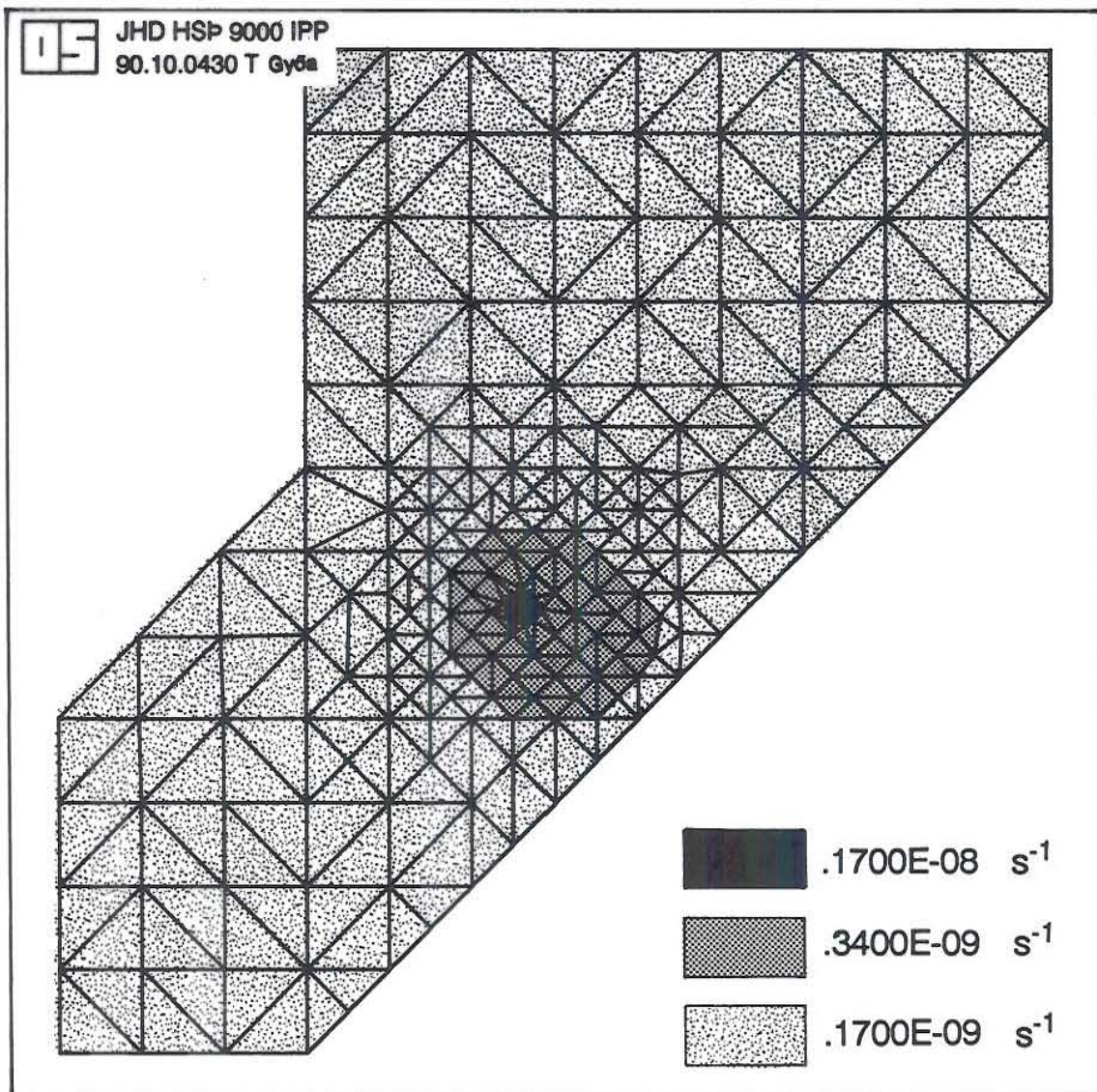
FIGURE 15: Map for leakage coefficient
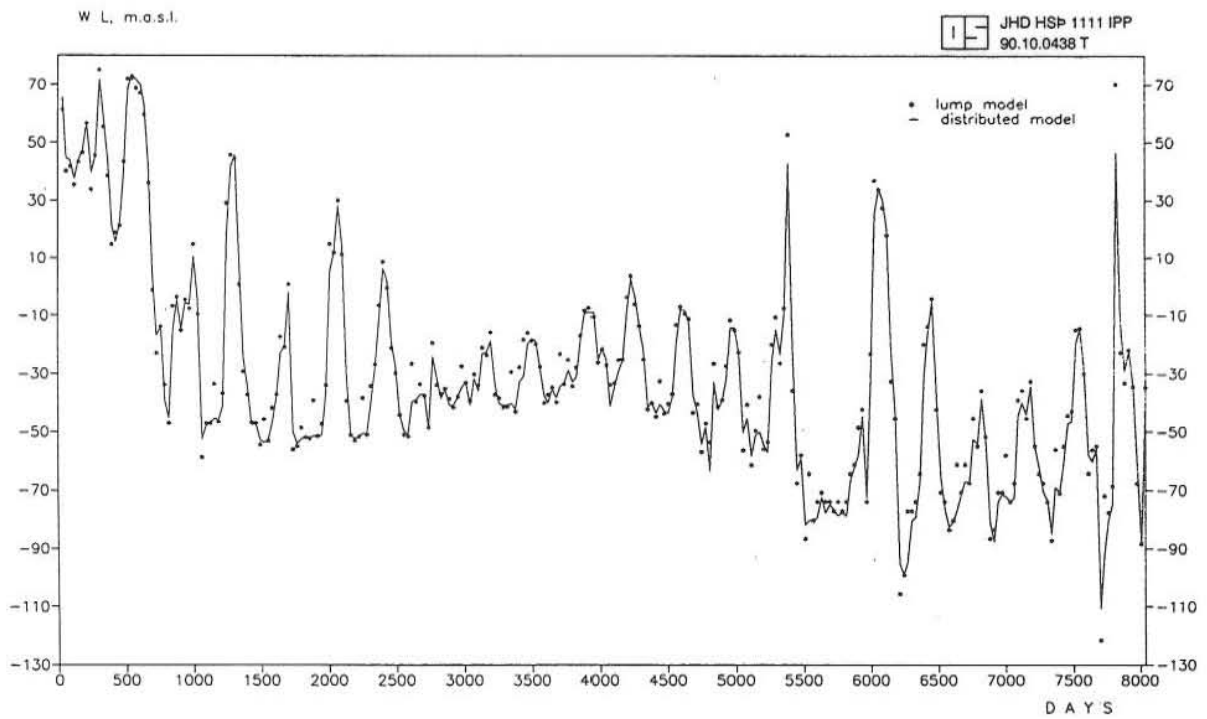
FIGURE 16: Water level changes - lumped and distributed models
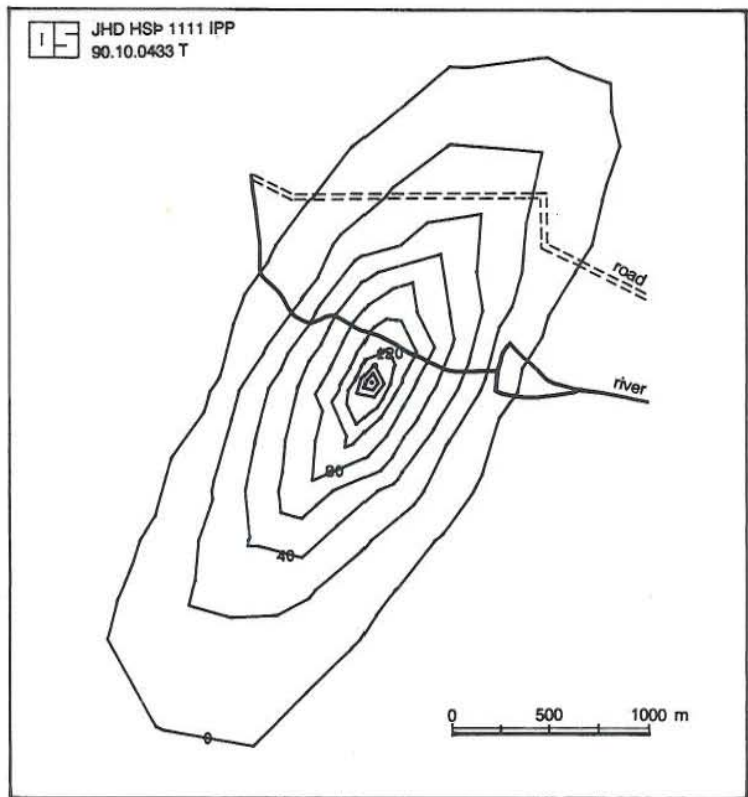
FIGURE 17: Area distribution of the drawdown
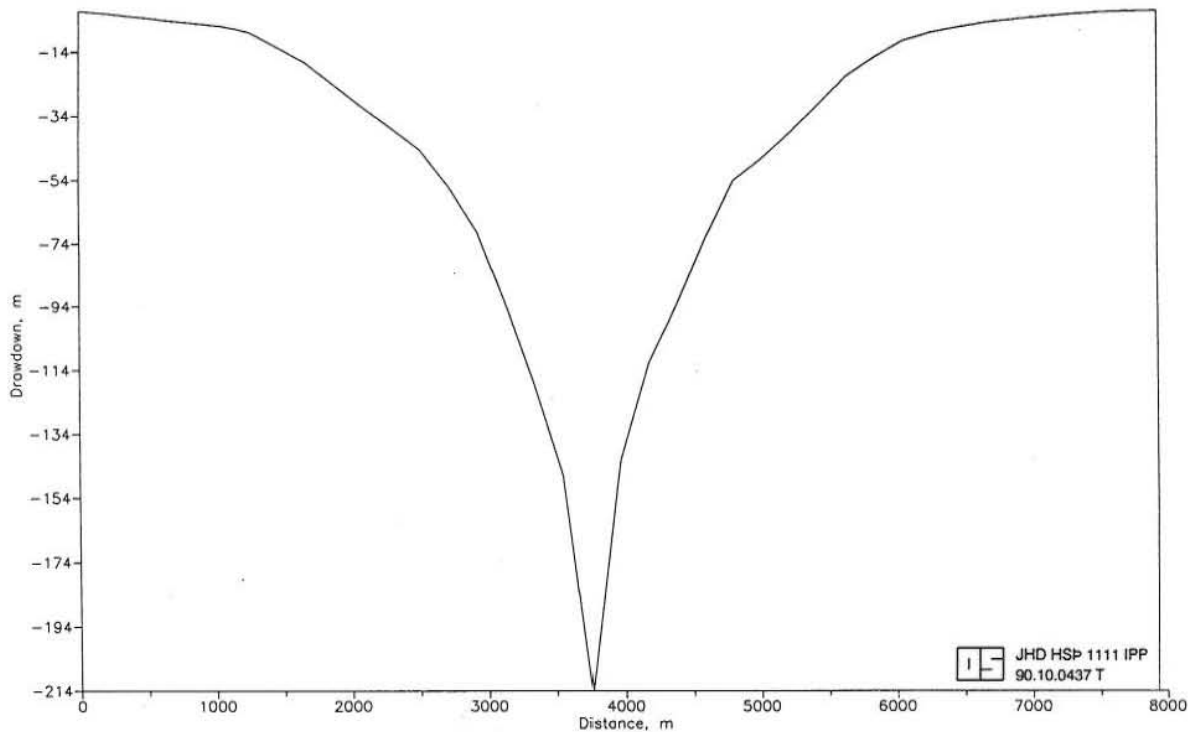
FIGURE 18: Cross-section of the drawdown

3.3.3.2 Mass problem

As the AQUA programme is also capable of solving the mass and heat transport problems, it is also used for modelling those conditions in the Ellidaár geothermal field. The result for the time-dependant solution is shown in Figure 19. Compared to the lumped model, it shows a rather rapid decline in the first years of production and a flattening of the process during the later stages. Together with the results of the lumped model, they fit pretty well with the field measurements of all the wells.

The mass balance for SiO_2 around the production area is given by the following equation:

$$QC = Q_b C_b + (Q - q_l)C_o \qquad (32)$$

The physical meaning of this equation is that the mass coming out of the geothermal reservoir with production (QC) should be equal to the mass entering it through boundaries ($Q_b C_b$) and leakage $[(Q - q_l)C_o]$. The values for C, Q_b, C_b and q_l (some are taken from the mass transport output files of AQUA) are as follows:

$$
\begin{aligned}
Q &= 126 \text{ l/s (average field production)} \\
C &= 60 \text{ mg/l (concentration in the production well)} \\
Q_b C_b &= 7.31 \text{ mg/s (mass flux through the well boundary, Appendix: Table 7)} \\
q_l &= 111 \text{ l/s (flow through the well boundary)} \\
C_o &= 20 \text{ mg/l (concentration in the upper layer)}
\end{aligned}
$$
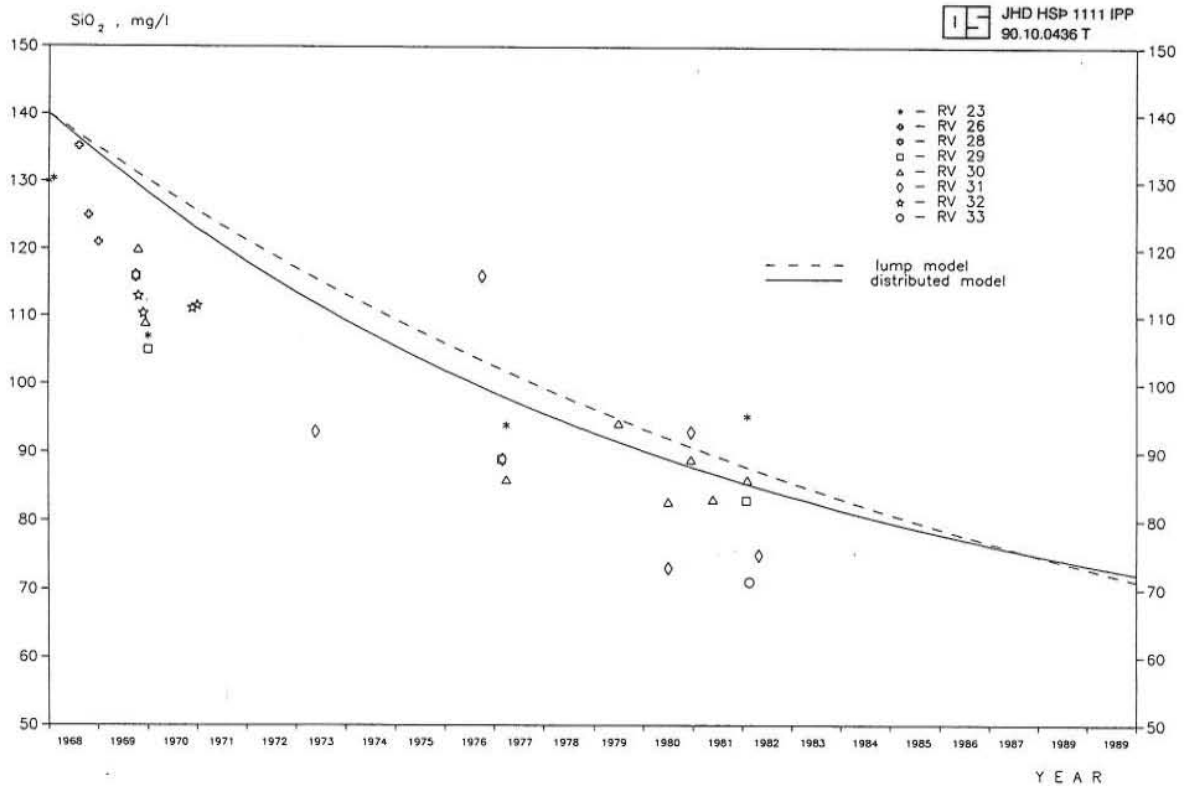
FIGURE 19: Mass transport - lumped and distributed models

Expressed in values, Equation 32 can be written as:

$$0.126 \times 60.00 = 7.31 + 20.00 \times 0.015$$

$$7.57 \approx 7.61$$

The area distribution of the SiO_2 decline can be seen in Figure 20 (Appendix: Table 8). It does not extend far away from the production zone and reaches its maximum of about 80 mg/l around the main producing wells.

3.3.3.3 Heat problem

As this problem is solved in a similar way to that of mass transport, we are not going into further details except to mention the existing differences between the two solutions. While the retardation constant (β) for handling the mass equation is $\beta = 0$, for the heat equation it is:

$$\beta = \frac{c_s}{c_w} = 0.21$$

The other change is the parameter for the vertical inflow (T_o); it is two times lower than the one we used for solving the mass problem.
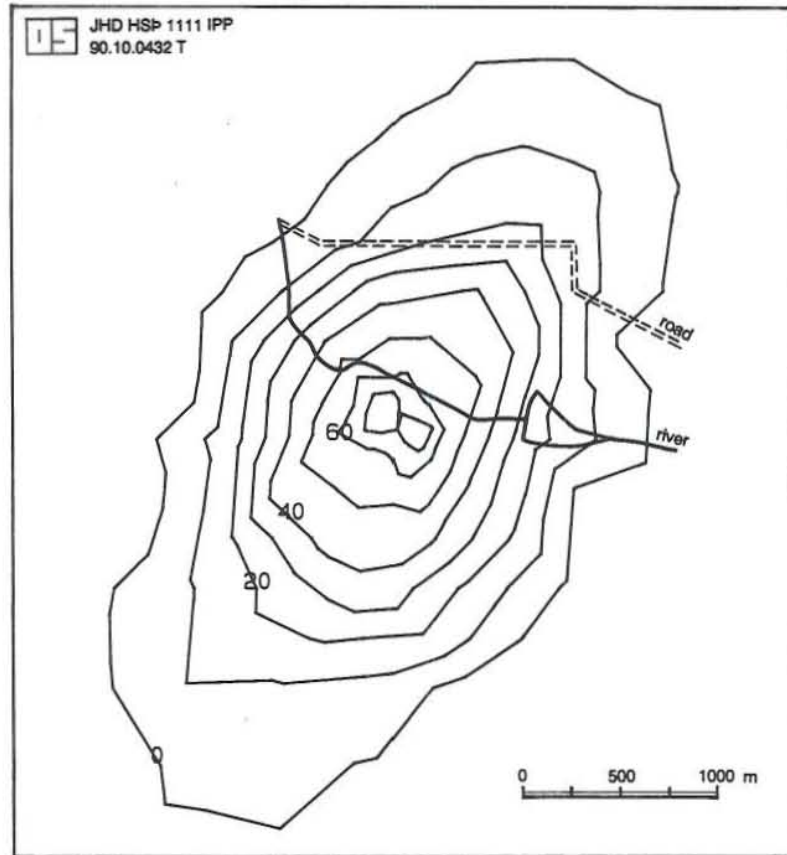
FIGURE 20: Area distribution of the changes in silica concentration (mg/l)

The balance equation concerning the preservation of heat can be written as follows:

$$QT = Q_b T_b + (Q - q_l)T_o \tag{33}$$

Its physical grounds are similar to those of the mass transport, already explained in the previous chapter. The values for T, Q_b, T_b, and q_l are taken from the flow across boundaries AQUA output files and are as follows:

T	=	72.59 °C (temperature in the production well)
$Q_b T_b$	=	9.10 m³ .°C/s (heat flux through the well boundary; Appendix: Table 9)
T_o	=	10.00 °C (temperature in the upper layer)
Q, q_l	=	as in Equation 32

Expressed in numbers, Equation 33 gives:

$$0.126 \times 72.59 = 9.10 + 0.015 \times 10$$

$$9.17 \approx 9.25$$

The values are close enough to be in agreement.

The heat transport decline curve is shown in Figure 21 (Appendix: Table 10). It almost overlaps
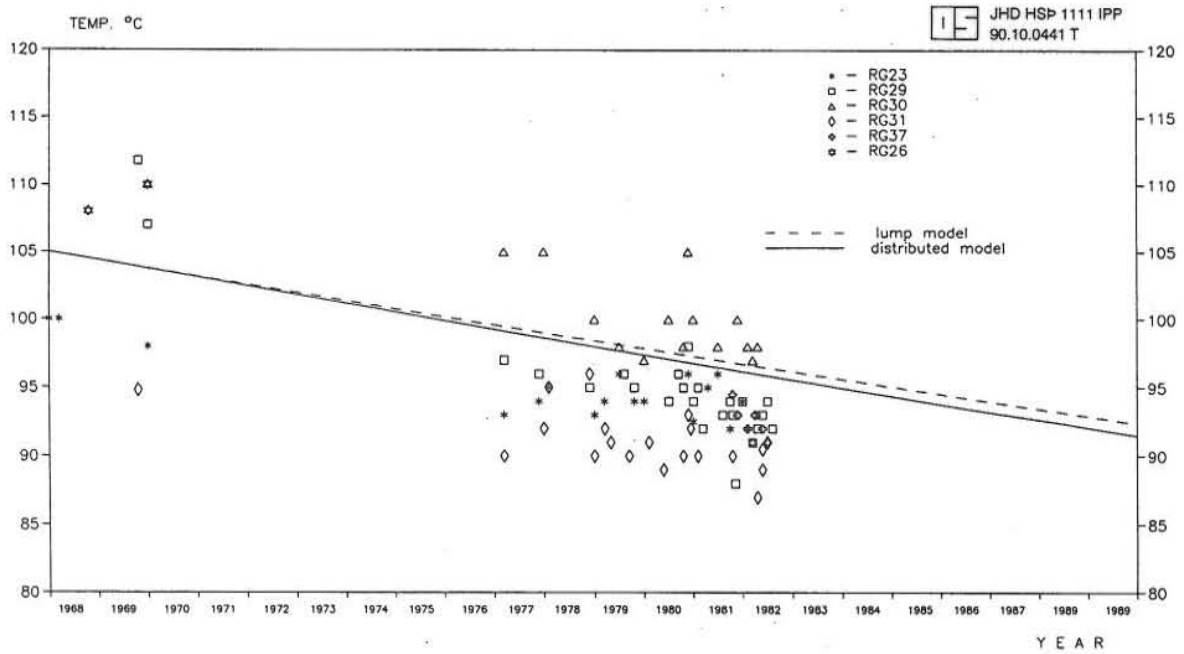
FIGURE 21: Heat transport - lumped and distributed models

that of the lumped model and fits quite well with the measurements. The area distribution of the reservoir cooling (Figure 22) shows that not too big an area is affected by it.

The energy that can be extracted from the field, using the average production of 126 l/s and a temperature drop of 50°C (Figure 23) is given by:

$$E = \rho_w c_w Q \Delta T = 27 \text{ MW}_{th}$$

The model parameters, used for solving the mass and heat transport and not mentioned yet, are as follows:

- longitudinal dispersivity (a_L)   = 20 m

- transversal dispersivity (a_T)   = 5 m

- sqrt(a_T/a_L)   = 0.5

- molecular diffusion   = 10^{-7} m² /s

- porosity (ϕ)   = 0.07

- aquifer thickness (b)   = 230 m

As can be seen, the values for porosity and aquifer thickness are lower than those calculated by the lumped model. The reason is that in the distributed model a greater area is involved, but altogether the multiplied value Abϕ is within acceptable limits for both models.
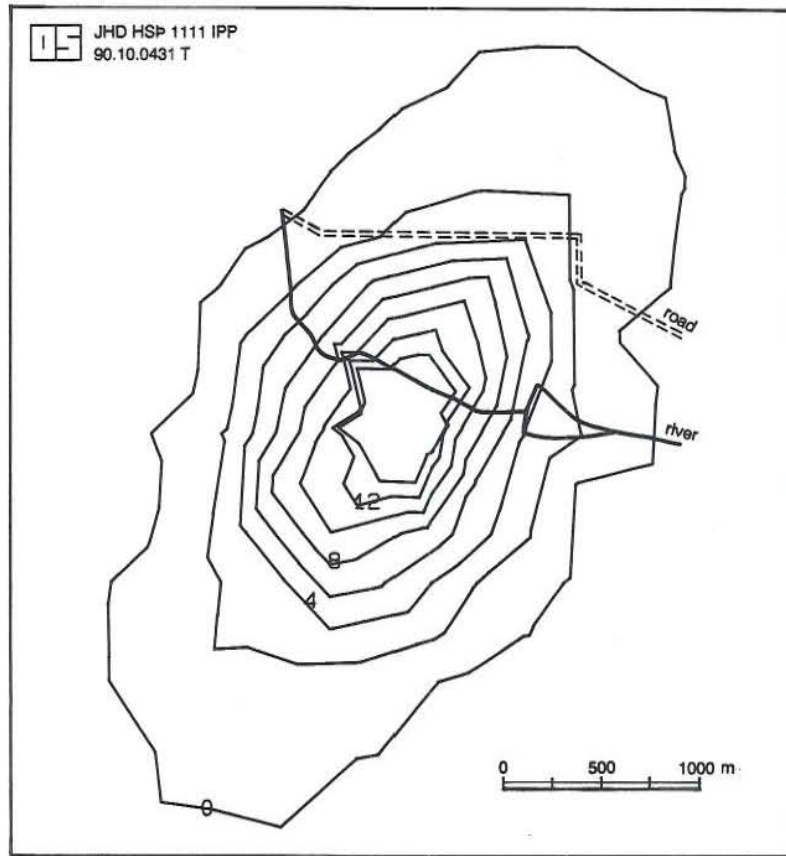
FIGURE 22: Area distribution of the reservoir cooling
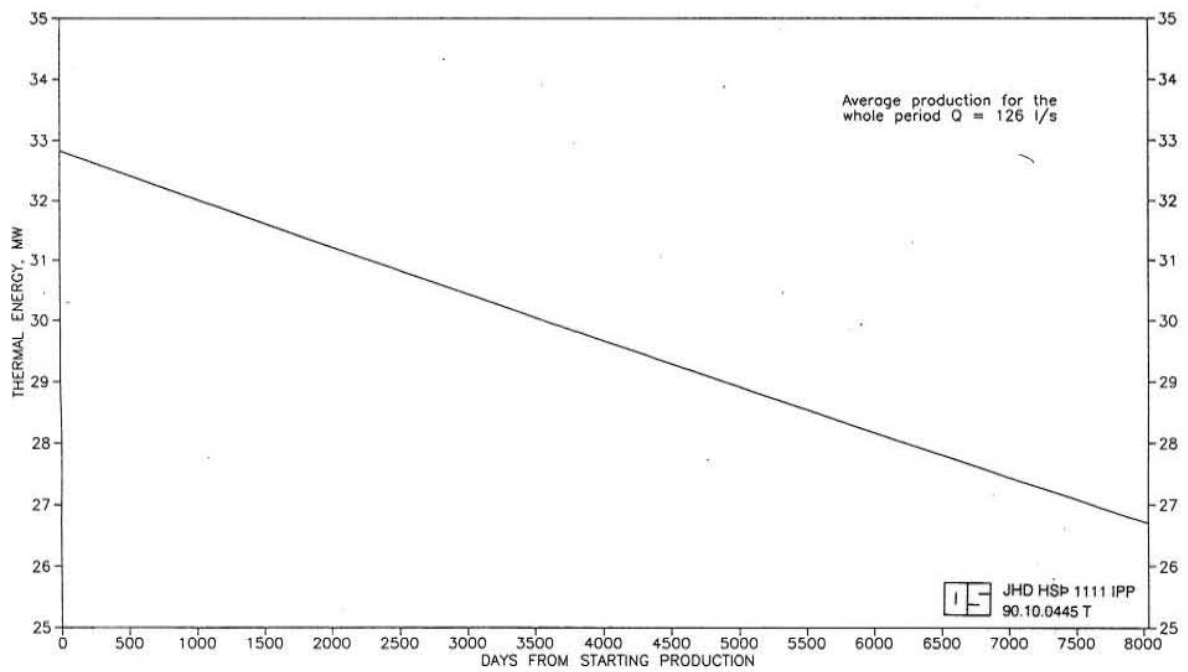
FIGURE 23: Decline of the extracted thermal energy with production

4. RESULTS AND CONCLUSIONS

The prime objective of this work is to create a model approximating the natural conditions of the Ellidaár geothermal reservoir, using the field data for the last 22 years. Through this model, the parameters and features of the field are described and some predictions of its future behaviour are made.

All available geological, geophysical and geochemical information, along with field measurement data were collected and carefully studied to understand how all these factors contributed to the overall picture of the geothermal reservoir. Two models were used for describing the effects due to production in the area.

The main characteristics of the Ellidaár geothermal reservoir can be stated as follows:

a. It lies in the vicinity of the Krisuvik fissure swarm, which extends out of the main volcanic zone in a general north-northeasterly direction. The geothermal reservoir is mainly connected with the hyaloclastite geological unit of the region. The main features in it are the fissures, faults and fractures which play a very important role in the hydrology of the region. The reservoir's permeability is mainly attributed to these geological phenomena.

b. The size of the production field is not big - about 0.8 km^2 , with impermeable boundaries along its northern and western parts and flow boundaries elsewhere. Resistivity measurements indicate a recharge of fresh (cold and low mineralized) water coming from a south and southeasterly direction.

c. The measurements from the field prior to the start of production, indicate higher initial values of SiO_2 and temperature. Over the production period of 22 years, the effects of water discharge are very clearly observed with a lowering of the water level, and a decline both in the SiO_2 content and temperature.

d. Two models are discussed in the report, one lumped and one distributed. Using the field data for production from the field, the results from the lumped model show very good matching with the measurements made during the whole calibration period of 8036 days, since the start of production. The calculated parameters are as follows:

$S = 1.6 \times 10^{-3}$, URF $= 0.833$ m/(l/s), $A = 0.8$ km^2, $K = 1062720$ s,

$k = 1.5 \times 10^{-7}$ m/s, $m = 100$ m, $b = 1000$ m, $\phi = 0.1$, $s = 105$ m.

The prediction shows a change in the water level with different production rates. A rise of about 80 m will occur, if the average annual production drops to 50 l/s. Because of the low value of the timeconstant, steady-state conditions are reached in a very short time.

e. The distributed model created by the AQUA programme examines more closely the reservoir properties and their lateral changes. The obtained results fit very adequately with those from measurements and the lumped model. They are as follows:

$S = 1.4 \times 10^{-3}$, $T_{xx} = 1.3 \times 10^{-3}$ m^2 /s, $T_{yy} = 1.3 \times 10^{-4}$ m^2 /s,

$k/m = 1.7 \times 10^{-9}$ s^{-1}, $A = 5 \times 10^4$ m^2, $b = 220$ m, $\phi = 0.07$,

flow across a well boundary $= 111.4$ l/s,

mass flux = 7.3 g/s, heat flux = 9.1 m³ °C/s,

thermal energy = 27 MW_{th}.

f. It may be noted that due to cooling of the geothermal reservoir, the losses of the extracted energy from the water are about 6 MW. One possible way to overcome this problem is to include a "loop" reinjection scheme in the production cycle. Thus, the reservoir pressure should be kept as high as possible, preventing the downflow of the cold water from the upper aquifer.

g. The predictions made by the models show what period of time is needed for recovering the initial values of SiO_2 and temperature in the geothermal reservoir if production stops right now. Taking into account the natural recharge into it (q_o = 15 l/s), this time is estimated to be about 160 years. On the other hand, if we want to prevent further mass and heat decline and keep them at the present level, the average annual production from the field should not exceed 20 l/s.

5. RECOMMENDATIONS

The study of the Ellidaár geothermal reservoir, applying the lumped and distributed models, presents results that are very close to the measured field data. This indicates a correct approach and indicates that both models are reliable for similar reservoir modelling and future forecasting. However, as the methods use only linear functions in their mathematical models, the effects of turbulence and skin impact are not taken into account. This means that the drawdown values in close proximity to the pumping wells cannot always be considered accurate.

As reinjection is one possible way to diminish the effects of drawdown (mass and heat decline), it must be considered and introduced in the future, especially if production is kept at the present rate.

It is recommended that field measurements of water level, silica content and temperature be carried out on a more regular basis. Although the models have matched very well with the field data for the measured period, a comparison for the whole production period would have been preferable.

In conclusion it can be said that, as a whole, the obtained results from both models are quite reasonable. As the distributed model gives a more accurate and complete picture of the aquifer, it is recommended that geothermal reservoirs of this kind are approached and solved in a similar way using the contemporary scientific art of the programme AQUA.

ACKNOWLEDGEMENTS

NOMENCLATURE

a_L : Longitudinal dispersivity, m
a_T : Transversal dispersivity, m
A   : Production area, m^2
b   : Thickness of the geothermal reservoir, m
c_s : Heat capacity of solid matrix = 900 J/kg.°C
c_w : Heat capacity of the water = 4190 J/kg.°C
C   : Concentration in the geothermal aquifer, mg/l
$C_b Q_b$: Mass flux, g/l
C_f : URF constant, m/(l/s)
C_i : Initial concentration in the geothermal reservoir = 140 mg/l
C_o : Concentration in vertical inflow = 20 mg/l
D_m : Molecular (heat) diffusivity, m^2 /s
e   : Exponential integral
E   : Extracted energy, W
F(t)   : Unit response function, m/(l/s)
h   : Potential in geothermal aquifer, m
h_o : Potential in upper aquifer, m
k   : Permeability of the aquitard, m/s
k_d : Distribution coefficient
k/m   : Leakage coefficient, s^{-1}
K   : Timeconstant, s
m   : Thickness of the aquitard, m
R_h : Retardation coefficient
q   : Leakage, m^3 /s
q_o : Recharge into the geothermal reservoir, m^3 /s
q_l : Flow through well boundary, m^3 /s
Q   : Production, m^3 /s
s   : Drawdown, m
S   : Storage coefficient
t   : Time, s
T   : Temperature in geothermal reservoir, °C
$T_b Q_b$: Heat flux, m^3 .°C/s
T_i : Initial temperature in the geothermal reservoir, °C
T_o : Temperature in the vertical inflow, °C

Greek letters:

β : Retardation constant;
γ : $k/m(h_o - h)$, m/s;
λ : Exponential decay constant, s^{-1};
μ : Upstream weighting factor;
ρ_s : Density of porous media = 2500 kg/m^3 ;
ρ_w : Density of thermal water = 951 kg/m^3 ;
ϕ : Porosity.

REFERENCES

Axelsson, G., 1989: Simulation of pressure response data from geothermal reservoirs by lumped parameter models. 14th Workshop on Geothermal Reservoir Engineering, Stanford, USA, in print.

Bodvarsson, G. and Witherspoon, P., 1989: Geothermal reservoir engineering - part 1. Lawrence Berkeley Laboratory, 1-30.

Georgsson, L.S., 1985: The Reykjavik - Borgarfjördur area, results of resistivity soundings. Orkustofnun, Reykjavik, report OS-85111/JHD-14 (in Icelandic), 41 pp.

Kjaran, S. P. and Eliasson, J., 1983: Geothermal reservoir engineering lecture notes. UNU Geothermal Training Programme, Iceland, report 2, 250 pp.

Kjaran, S., 1986: Geothermal reservoir engineering experience in Iceland. Nordic Hydrol., 17, 417-438.

Penev, I., 1990: Appendix to the report: Lumped and distributed models of the Ellidaár geothermal field, SW-Iceland. UNU G.T.P., Iceland, report 12 appendix, 21 pp.

Smarason, O.B., Tomasson, J. and Ganda, S., 1989: Alteration mineralogy of the Ellidaár geothermal field, Reykjavik, Iceland. Water-Rock Interaction WRI-6. In, Miles, D. L. (editor): Proceedings of the 6th International Symposium on Water-Rock Interaction, 643-646.

Tomasson, J., 1990: The Ellidaár geothermal area, nature and response to production. Report, unpublished.

Tomasson, J., Fridleifsson, I. B. and Stefansson, V., 1975: A hydrological model for the flow of thermal water in southwestern Iceland with special reference to the Reykir and Reykjavik thermal areas. 2nd UNU symposium on the developement and use of geothermal resources, San Francisco, Proceedings, 643-648.

Vatnaskil Consulting Engineers 1989: AQUA manual. Vatnaskil, Reykjavik.

Reykjavik District Heating Services and Vatnaskil Consulting Engineers, 1982a: Report to Hitaveita Reykjavikur. Report (in Icelandic), 08.1982.

Reykjavik District Heating Services and Vatnaskil Consulting Engineers, 1982b: Report to Hitaveita Reykjavikur. Report (in Icelandic), 12.1982.

APPENDIX TO THE REPORT:
LUMPED AND DISTRIBUTED MODELS OF THE ELLIDAÁR GEOTHERMAL FIELD, SW-ICELAND

Ivan Penev,
UNU Geothermal Training Programme,
Orkustofnun - National Energy Authority,
Grensasvegur 9,
108 Reykjavik,
ICELAND

Permanent address:
New Energy Sources,
Stud. grad, "V.Gentchev" 51,
Sofia,
BULGARIA

This is the appendix to the report : Lumped and distributed models of the Ellidaár geothermal field, SW-Iceland. It was written by Ivan Penev at the UNU Geothermal Training Programme in 1990. It includes 10 different tables with production data and results of calculations. The contents are listed below.

LIST OF TABLES PUBLISHED IN THIS APPENDIX

TABLE 1: Production from the field during the period 1968-1989

YEAR	MONTH	No OF MONTHS	PRODUCT. m3/m	DAYS	PRODUCT. l/s
1	2	3	4	5	6
	1	1	43000	31	16.054
	2	2	110000	60	43.902
	3	3	105000	91	39.203
	4	4	125000	121	48.225
	5	5	100000	152	37.336
	6	6	90000	182	34.722
1968	7	7	58000	213	21.655
	8	8	130000	244	48.536
	9	9	93000	274	35.880
	10	10	0	305	0.000
	11	11	62000	335	23.920
	12	12	114990	366	42.932
		total m3/m	1030990	average l/s	32.697
	1	13	190260	397	71.035
	2	14	177550	425	73.392
	3	15	169340	456	63.224
	4	16	99950	486	38.561
	5	17	9691	517	3.618
	6	18	9379	547	3.618
1969	7	19	19840	578	7.407
	8	20	24930	609	9.308
	9	21	47910	639	18.484
	10	22	123000	670	45.923
	11	23	240820	700	92.909
	12	24	309320	731	115.487
		total m3/m	1421990	average l/s	45.247
	1	25	280390	762	104.686
	2	26	343712	790	142.077
	3	27	384893	821	143.703
	4	28	258056	851	99.559
	5	29	247922	882	92.563
	6	30	284579	912	109.791
1970	7	31	250900	943	93.675
	8	32	260640	974	97.312
	9	33	190110	1004	73.345
	10	34	267020	1035	99.694
	11	35	422210	1065	162.890
	12	36	385510	1096	143.933
		total m3/m	3575942	average l/s	113.602

1	2	3	4	5	6
	1	37	385050	1127	143.761
	2	38	342750	1155	141.679
	3	39	383530	1186	143.194
	4	40	352940	1216	136.165
	5	41	144810	1247	54.066
	6	42	92620	1277	35.733
1971	7	43	96500	1308	36.029
	8	44	234140	1339	87.418
	9	45	328850	1369	126.871
	10	46	354160	1400	132.228
	11	47	384220	1430	148.233
	12	48	384840	1461	143.683
	total m3/m		3484410	average l/s	110.755
	1	49	408240	1492	152.419
	2	50	380838	1521	151.995
	3	51	404332	1552	150.960
	4	52	368490	1582	142.164
	5	53	353710	1613	132.060
	6	54	291530	1643	112.473
1972	7	55	302810	1674	113.056
	8	56	233860	1705	87.313
	9	57	413620	1735	159.576
	10	58	409953	1766	153.059
	11	59	390077	1796	150.493
	12	60	400430	1827	149.503
	total m3/m		4357890	average l/s	137.923
	1	61	401680	1858	149.970
	2	62	360260	1886	148.917
	3	63	399210	1917	149.048
	4	64	385950	1947	148.900
	5	65	343850	1978	128.379
	6	66	189565	2008	73.135
1973	7	67	199195	2039	74.371
	8	68	141840	2070	52.957
	9	69	201100	2100	77.585
	10	70	361020	2131	134.789
	11	71	397870	2161	153.499
	12	72	403930	2192	150.810
	total m3/m		3785470	average l/s	120.197

1	2	3	4	5	6
	1	73	399660	2223	149.216
	2	74	357870	2251	147.929
	3	75	397760	2282	148.507
	4	76	344840	2312	133.040
	5	77	321320	2343	119.967
	6	78	257170	2373	99.217
1974	7	79	209230	2404	78.118
	8	80	238120	2435	88.904
	9	81	303840	2465	117.222
	10	82	331030	2496	123.592
	11	83	376030	2526	145.073
	12	84	397610	2557	148.451
	total m3/m		3934480	average l/s	124.936
	1	85	399600	2588	149.194
	2	86	320650	2616	132.544
	3	87	361710	2647	135.047
	4	88	343010	2677	132.334
	5	89	355490	2708	132.725
	6	90	389820	2738	150.394
1975	7	91	298291	2769	111.369
	8	92	343800	2800	128.360
	9	93	353470	2830	136.370
	10	94	347780	2861	129.846
	11	95	358810	2891	138.430
	12	96	367910	2922	137.362
	total m3/m		4240341	average l/s	134.498
	1	97	356420	2953	133.072
	2	98	323490	2982	129.107
	3	99	341400	3013	127.464
	4	100	360950	3043	139.255
	5	101	332170	3074	124.018
	6	102	344111	3104	132.759
1976	7	103	303305	3135	113.241
	8	104	311462	3166	116.287
	9	105	286683	3196	110.603
	10	106	354090	3227	132.202
	11	107	357740	3257	138.017
	12	108	367610	3288	137.250
	total m3/m		4039431	average l/s	127.773

1	2	3	4	5	6
	1	109	366850	3319	136.966
	2	110	329430	3347	136.173
	3	111	372660	3378	139.135
	4	112	324250	3408	125.096
	5	113	294670	3439	110.017
	6	114	287200	3469	110.802
1977	7	115	295790	3500	110.435
	8	116	299416	3531	111.789
	9	117	323911	3561	124.966
	10	118	362933	3592	135.504
	11	119	354191	3622	136.648
	12	120	346459	3653	129.353
	total m3/m		3957760	average l/s	125.574
	1	121	361970	3684	135.144
	2	122	310200	3712	128.224
	3	123	342690	3743	127.946
	4	124	316192	3773	121.988
	5	125	344958	3804	128.793
	6	126	324830	3834	125.320
1978	7	127	290019	3865	108.281
	8	128	262921	3896	98.163
	9	129	259716	3926	100.199
	10	130	269571	3957	100.646
	11	131	319210	3987	123.152
	12	132	304752	4018	113.781
	total m3/m		3707029	average l/s	117.636
	1	133	322176	4049	120.287
	2	134	343436	4077	141.963
	3	135	341794	4108	127.611
	4	136	316502	4138	122.107
	5	137	315860	4169	117.929
	6	138	248121	4199	95.726
1979	7	139	224791	4230	83.927
	8	140	255669	4261	95.456
	9	141	279763	4291	107.933
	10	142	316138	4322	118.032
	11	143	369941	4352	142.724
	12	144	362866	4383	135.479
	total m3/m		3697057	average l/s	117.431

1	2	3	4	5	6
	1	145	377966	4414	141.116
	2	146	339631	4443	135.549
	3	147	374603	4474	139.861
	4	148	364074	4504	140.461
	5	149	353400	4535	131.944
	6	150	278491	4565	107.443
1980	7	151	258654	4596	96.570
	8	152	266080	4627	99.343
	9	153	272000	4657	104.938
	10	154	373616	4688	139.492
	11	155	364284	4718	140.542
	12	156	416435	4749	155.479
	total m3/m		4039234	average l/s	127.728
	1	157	385253	4780	143.837
	2	158	405802	4808	167.742
	3	159	320419	4839	119.631
	4	160	367130	4869	141.640
	5	161	359814	4900	134.339
	6	162	323080	4930	124.645
1981	7	163	273411	4961	102.080
	8	164	284009	4992	106.037
	9	165	308465	5022	119.007
	10	166	414455	5053	154.740
	11	167	364851	5083	140.760
	12	168	430642	5114	160.783
	total m3/m		4237331	average l/s	134.603
	1	169	393388	5145	146.874
	2	170	356460	5173	147.346
	3	171	413124	5204	154.243
	4	172	405438	5234	156.419
	5	173	300000	5265	112.007
	6	174	270000	5295	104.167
1982	7	175	320000	5326	119.474
	8	176	260000	5357	97.073
	9	177	70000	5387	27.006
	10	178	350000	5418	130.675
	11	179	450000	5448	173.611
	12	180	420000	5479	156.810
	total m3/m		4008410	average l/s	127.142

1	2	3	4	5	6
	1	181	510000	5510	190.412
	2	182	440000	5538	181.878
	3	183	490000	5569	182.945
	4	184	470000	5599	181.327
	5	185	460000	5630	171.744
	6	186	470000	5660	181.327
1983	7	187	470000	5691	175.478
	8	188	480000	5722	179.211
	9	189	470000	5752	181.327
	10	190	480000	5783	179.211
	11	191	470000	5813	181.327
	12	192	440000	5844	164.277
	total	m3/m	5650000	average l/s	179.206
	1	193	430000	5875	160.544
	2	194	390000	5904	155.651
	3	195	370000	5935	138.142
	4	196	470000	5965	181.327
	5	197	310000	5996	115.741
	6	198	120000	6026	46.296
1984	7	199	130000	6057	48.536
	8	200	150000	6088	56.004
	9	201	180000	6118	69.444
	10	202	340000	6149	126.941
	11	203	380000	6179	146.605
	12	204	570000	6210	212.814
	total	m3/m	3840000	average l/s	121.504
	1	205	550000	6241	205.346
	2	206	480000	6269	198.413
	3	207	480000	6300	179.211
	4	208	470000	6330	181.327
	5	209	440000	6361	164.277
	6	210	300000	6391	115.741
1985	7	211	280000	6422	104.540
	8	212	250000	6453	93.339
	9	213	370000	6483	142.747
	10	214	460000	6514	171.744
	11	215	470000	6544	181.327
	12	216	500000	6575	186.679
	total	m3/m	5050000	average l/s	160.391

1	2	3	4	5	6
	1	217	490000	6606	182.945
	2	218	430000	6634	177.745
	3	219	460000	6665	171.744
	4	220	430000	6695	165.895
	5	221	450000	6726	168.011
	6	222	380000	6756	146.605
1986	7	223	410000	6787	153.076
	8	224	350000	6818	130.675
	9	225	400000	6848	154.321
	10	226	510000	6879	190.412
	11	227	500000	6909	192.901
	12	228	460000	6940	171.744
	total m3/m		5270000	average l/s	167.173
	1	229	460000	6971	171.744
	2	230	420000	6999	173.611
	3	231	470000	7030	175.478
	4	232	450000	7060	173.611
	5	233	360000	7091	134.409
	6	234	350000	7121	135.031
1987	7	235	380000	7152	141.876
	8	236	340000	7183	126.941
	9	237	410000	7213	158.179
	10	238	440000	7244	164.277
	11	239	450000	7274	173.611
	12	240	470000	7305	175.478
	total m3/m		5000000	average l/s	158.687
	1	241	511886	7336	191.116
	2	242	413848	7365	165.169
	3	243	460901	7396	172.081
	4	244	410441	7426	158.349
	5	245	376838	7457	140.695
	6	246	372510	7487	143.715
1988	7	247	284144	7518	106.087
	8	248	282406	7549	105.438
	9	249	331458	7579	127.877
	10	250	439532	7610	164.102
	11	251	414360	7640	159.861
	12	252	410173	7671	153.141
	total m3/m		4708497	average l/s	148.969

1	2	3	4	5	6
	1	253	620486	7702	231.66
	2	254	463730	7730	191.69
	3	255	481695	7761	179.84
	4	256	453468	7791	174.95
	5	257	15115	7822	5.64
	6	258	308799	7852	119.14
1989	7	259	341600	7883	127.54
	8	260	306090	7914	114.28
	9	261	345883	7944	133.44
	10	262	450326	7975	168.13
	11	263	515970	8005	199.06
	12	264	332204	8036	124.03
	total m3/m		4635366	average l/s	147.45

Total production for the period 68 - 89		m3	87671628	av. for the period l/s	126.27

PARAMETERS OF THE FIELD:

Time for production	yr	22
	mnt	264
Area of reservoir	m2	0.8E6
Thickness of aquitard	m	100
Thickness of reserv.	m	1000
Permeability of aquit.	m/s	1.5E-7
Storage coeff. of reserv.	--	1.6E -3
Timeconstant prod.	day	12.3
conc.	yr	20.07
temp.	yr	132.5
U R F	m(l/s)	0.833

Recharge	l/s	15
Porosity	--	0.1
Density of water	kg/m3	951
matrix	kg/m3	2500
Heat capacity of water	J/kg/oC	4190
matrix	J/kg/oC	1000
Retardation coefficient	- -	6.6
SiO2 conc. in cold aq.	mg/l	20
in th. aq.	mg/l	140
Temperature in cold aq.	oC	10
in th. aq.	oC	105

TABLE 2: Prediction for water level change with different production for 1990-2000

MONTHS	DAYS	PRODUCT.	PRODUCT.	DRAWDOWN	W A S L
-	-	m3/m	l/s	m	m
1	2	3	4	5	6
AVERAGE PRODUCTION: 147 l/s					
1	31	620486	231.66		
2	28	463730	191.69		
3	31	481695	179.84		
4	30	453468	174.95		
5	31	15115	5.64		
6	30	308799	119.14	109.9	-34.9
7	31	341600	127.54		
8	31	306090	114.28		
9	30	345883	133.44		
10	31	450326	168.13		
11	30	515970	199.06		
12	31	332204	124.03		
		TOTAL 4635366	AVER.147.45		
AVERAGE PRODUCTION: 126 l/s					
1	31	531363	198.39		
2	28	397123	164.15		
3	31	412507	154.01		
4	30	388334	149.82		
5	31	12944	4.83		
6	30	264445	102.02	92.7	-17.7
7	31	292535	109.22		
8	31	262125	97.87		
9	30	296202	114.28		
10	31	385644	143.98		
11	30	441859	170.47		
12	31	284488	106.22		
		TOTAL 3969569	AVER.126.27		

AVERAGE PRODUCTION: 100 l/s

1	31	422099	157.59		
2	28	315463	130.40		
3	31	327684	122.34		
4	30	308482	119.01		
5	31	10282	3.84		
6	30	210067	81.04	70.8	4.2
7	31	232381	86.76		
8	31	208224	77.74		
9	30	235295	90.78		
10	31	306344	114.38		
11	30	351000	135.42		
12	31	225989	84.37		

TOTAL 3153310   AVER.100.31

AVERAGE PRODUCTION: 75 l/s

1	31	315606	117.83		
2	28	235873	97.50		
3	31	245011	91.48		
4	30	230654	88.99		
5	31	7688	2.87		
6	30	157069	60.60	50	25
7	31	173753	64.87		
8	31	155691	58.13		
9	30	175931	67.87		
10	31	229055	85.52		
11	30	262445	101.25		
12	31	168973	63.09		

TOTAL 2357749   AVER. 75.00

AVERAGE PRODUCTION: 50 l/s

1	31	210404	78.56		
2	28	157249	65.00		
3	31	163341	60.98		
4	30	153769	59.32		
5	31	5125	1.91		
6	30	104712	40.40	29.2	45.8
7	31	115835	43.25		
8	31	103794	38.75		
9	30	117287	45.25		
10	31	152704	57.01		
11	30	174963	67.50		
12	31	112649	42.06		

TOTAL 1571832   AVER. 50.00

TABLE 3:   Mass and heat changes during the production period 1968-1989

YEAR	SIO2	TEMP
-	mg/l	oC
1968	140.00	105.00
1969	134.976	104.38
1970	130.195	103.764
1971	125.647	103.152
1972	121.321	102.546
1973	117.204	101.944
1974	113.288	101.346
1975	109.562	100.753
1976	106.017	100.164
1977	102.644	99.5804
1978	99.4354	99.0006
1979	96.3826	98.4252
1980	93.4782	97.8541
1981	90.715	97.2873
1982	88.086	96.7248
1983	85.5849	96.1665
1984	83.2053	95.6124
1985	80.9414	95.0624
1986	78.7875	94.5166
1987	76.7383	93.9749
1988	74.7887	93.4373
1989	72.9339	92.9037
1990	71.1692	92.3741

TABLE 4: Prediction for SiO_2 change during the period 1990-2000

YEAR	AVERAGE PRODUCTION, l/s						
	147	126	100	75	50	25	10
	CONTENT OF SIO2, mg/l						
1990	71.17	71.17	71.17	71.17	71.17	71.17	71.17
1991	68.69	69.4903	69.6067	70.0932	70.5876	71.0869	71.3888
1992	66.3501	67.893	68.1038	69.0478	70.0166	71.0046	71.6068
1993	64.1423	66.3733	66.6588	68.0329	69.4567	70.9231	71.8239
1994	62.0593	64.9275	65.2697	67.0476	68.9078	70.8425	72.0402
1995	60.0939	63.552	63.9342	66.091	68.3696	70.7626	72.2556
1996	58.2395	62.2433	62.6502	65.1623	67.8419	70.6835	72.4702
1997	56.4899	60.9982	61.4158	64.2607	67.3245	70.6051	72.6839
1998	54.839	59.8137	60.2291	63.3853	66.8173	70.5276	72.8968
1999	53.2815	58.6867	59.0882	62.5355	66.3199	70.4508	73.1088
2000	51.8118	57.6145	57.9913	61.7104	65.8322	70.3747	73.32

TABLE 5: Prediction for temperature change during the period 1990-2000

	AVERAGE PRODUCTION, l/s						
	147	126	100	75	50	25	10
YEAR	TEMPERATURE, oC						
1990	92.37	92.37	92.37	92.37	92.37	92.37	92.37
1991	91.7616	91.8485	91.9915	92.0842	92.2069	92.3298	92.40
1992	91.1288	91.3269	91.5855	91.7997	92.0443	92.2896	92.43
1993	90.5015	90.8092	91.1819	91.5165	91.8822	92.2495	92.47
1994	89.8796	90.2954	90.7807	91.2345	91.7205	92.2094	92.50
1995	89.2633	89.7854	90.3819	90.9538	91.5593	92.1694	92.53
1996	88.6523	89.2793	89.9855	90.6743	91.3987	92.1295	92.57
1997	88.0467	88.7769	89.5914	90.3961	91.2385	92.0896	92.60
1998	87.4464	88.2784	89.1997	90.1192	91.0787	92.0498	92.63
1999	86.8513	87.7836	88.8103	89.8435	90.9195	92.01	92.67
2000	86.2614	87.2925	88.4232	89.569	90.7607	91.9703	92.70

TABLE 6: Flow across boundary

Boundary no.   1

Node	Flow (L**3/S)	(L**3/S)/L
14	.8050121E-08	.9431304E-11
263	-.1003109E-07	-.1418611E-10
13	-.6327095E-08	-.8947864E-11
262	-.1251476E-05	-.1769855E-08
12	-.1518747E-05	-.2147832E-08
261	.2940784E-05	.4158897E-08
11	.1055668E-04	.1492940E-07
260	.8872894E-05	.1254817E-07
10	-.6834509E-05	-.9665456E-08
259	-.4110777E-05	-.5813517E-08
9	-.8209492E-05	-.1160997E-07
258	.6484367E-04	.9170280E-07
8	-.8791572E-05	-.1243316E-07
257	-.1625262E-04	-.2298467E-07
7	-.8821147E-04	-.1247499E-06
256	-.1785508E-04	-.2525090E-07
6	-.2085744E-04	-.2949687E-07
255	-.9540627E-05	-.1349248E-07
5	-.7231138E-05	-.8471805E-08
4	-.1591200E-04	-.1591200E-07
2	-.4582495E-05	-.4582495E-08
1	-.4356559E-07	-.4356559E-10

Total   -.1239973E-03   -.7412593E-08

Boundary no.   2

Node	Flow (L**3/S)	(L**3/S)/L
296	.4594888E-03	.4668285E-05
297	-.4549622E-01	-.4399981E-03
290	-.1024468E-01	-.1068764E-03
283	-.4830842E-02	-.4955009E-04
298	-.4571401E-02	-.3978492E-04
285	-.6737895E-02	-.5482463E-04
286	-.9611891E-02	-.9775721E-04
299	-.3039727E-01	-.3631001E-03

Total   -.1114307   -.1367214E-03

Accumulated total =   -.1115547

TABLE 7: Mass flux across boundary

YEAR	MASS FLUX (g/l) AROUND:	
	PROD.WELL	OUTER BOUND.
1968	-13.8965	-0.01876
1969	-12.96	-0.01874
1970	-12.2538	-0.01872
1971	-11.6759	-0.0187
1972	-11.1816	-0.01868
1973	-10.7481	-0.01867
1974	-10.3622	-0.01865
1975	-10.0155	-0.01863
1976	-9.70183	-0.01861
1977	-9.41664	-0.01859
1978	-9.15622	-0.01858
1979	-8.91755	-0.01856
1980	-8.6981	-0.01854
1981	-8.4957	-0.01852
1982	-8.30851	-0.0185
1983	-8.13493	-0.01849
1984	-7.97356	-0.01847
1985	-7.82319	-0.01845
1986	-7.68275	-0.01843
1987	-7.55129	-0.01842
1988	-7.42798	-0.0184
1989	-7.31209	-0.01838

TABLE 8: Change of SiO_2, calculated by AQUA

| YEAR | MASS DECLINE (mg/l) IN: | |
	OBS. WELL	PROD.WELL
1968	140.00	140.00
1969	134.02	117.01
1970	128.32	106.61
1971	123.01	100.07
1972	118.11	95.13
1973	113.58	91.03
1974	109.40	87.49
1975	105.56	84.37
1976	102.00	81.57
1977	98.72	79.05
1978	95.69	76.76
1979	92.87	74.67
1980	90.26	72.76
1981	87.84	71.01
1982	85.59	69.39
1983	83.49	67.90
1984	81.53	66.52
1985	79.70	65.24
1986	77.98	64.04
1987	76.38	62.93
1988	74.87	61.89
1989	73.45	60.91
1990	72.12	60.00

TABLE 9:   Heat flux across boundary

| YEAR | HEAT FLUX (m3/s/oC) AROUND | |
	PROD. WELL	OUTER BOUND.
1968	-11.2496	-0.01619
1969	-11.0486	-0.01619
1970	-10.8746	-0.01618
1971	-10.7195	-0.01618
1972	-10.5787	-0.01618
1973	-10.4494	-0.01618
1974	-10.3296	-0.01618
1975	-10.2178	-0.01617
1976	-10.1129	-0.01617
1977	-10.014	-0.01617
1978	-9.92017	-0.01617
1979	-9.83092	-0.01617
1980	-9.74568	-0.01617
1981	-9.664	-0.01616
1982	-9.58551	-0.01616
1983	-9.50989	-0.01616
1984	-9.43686	-0.01616
1985	-9.36617	-0.01616
1986	-9.29763	-0.01616
1987	-9.23105	-0.01615
1988	-9.16629	-0.01615
1989	-9.1032	-0.01615

TABLE 10: Change of temperature, calculated by AQUA

| YEAR | HEAT DECLINE (oC) IN: | |
	OBS. WELL	PROD.WELL
1968	105.00	105.00
1969	104.37	99.40
1970	103.73	95.26
1971	103.09	92.11
1972	102.45	89.63
1973	101.81	87.62
1974	101.16	85.93
1975	100.52	84.48
1976	99.88	83.21
1977	99.25	82.07
1978	98.62	81.04
1979	97.99	80.10
1980	97.38	79.22
1981	96.76	78.40
1982	96.15	77.63
1983	95.55	76.90
1984	94.95	76.21
1985	94.36	75.55
1986	93.78	74.91
1987	93.20	74.30
1988	92.63	73.71
1989	92.07	73.14
1990	91.51	72.59